APTD-0910

PB 206 411

THE TREATMENT OF METEOROLOGICAL VARIABLES

Appendix C

of

Development of a Simulation Model
for Estimating Ground Level Concentrations
of Photochemical Pollutants

Prepared by

Systems Applications, Inc.
Beverly Hills, California 90212

for the

Air Pollution Control Office
of the Environmental Protection Agency
Durham, North Carolina 27701

Reproduced by
NATIONAL TECHNICAL
INFORMATION SERVICE
Springfield, Va. 22151

BIBLIOGRAPHIC DATA SHEET	1. Report No. APTD-0910	2.	3. Recipient's Accession No.
4. Title and Subtitle Development of a Simulation Model for Estimating Ground Level Concentrations of Photochemical Pollutants - Appendix C: The Treatment of Meteorological Variables			5. Report Date June 1971 6.
7. Author(s) Philip M. Roth, Steven D. Reynolds, Philip J.W. Roberts			8. Performing Organization Rept. No. 71-SAI-17
9. Performing Organization Name and Address Systems Applications, Inc. Beverly Hills, California 90212			10. Project/Task/Work Unit No. 11. Contract/Grant No. CPA 70-148
12. Sponsoring Organization Name and Address Environmental Protection Agency Office of Air Programs Durham, North Carolina 27701			13. Type of Report & Period Covered 14.

15. Supplementary Notes

16. Abstracts

The preparation and conversion to digital form of contour maps of surface wind speed and direction (isotachs and streamlines, respectively) and of the height of the inversion base--in each case hourly representations, were achieved. Several approaches to the calculation of the wind field aloft, one of which appears to be a useful method for the automatic generation of these wind fields were also explored. For inversions, surface wind fields, winds aloft, and turbulent diffusivities for the days of validation, the following are described: the computational and data requirements; the nature of the available data base; efforts in satisfying the stated requirements; and the deficiencies in approach and, thus, recommended future efforts.

17. Key Words and Document Analysis. 17a. Descriptors

Air pollution
Simulation
Mathematical models
Photochemical reactions
Concentration (composition)
Mapping
Wind (meteorology)
Temperature inversion
Altitude
Data processing
Atmospheric diffusion
Urban areas

17b. Identifiers/Open-Ended Terms

17c. COSATI Field/Group 13B

18. Availability Statement	19. Security Class (This Report)	21. No. of Pages
Unlimited	UNCLASSIFIED	~~50~~ 51
	20. Security Class (This Page) UNCLASSIFIED	22. Price

FORM NTIS-38 (10-70)

USCOMM-DC 40329-P71

THE TREATMENT OF METEOROLOGICAL VARIABLES

Appendix C

of

Development of a Simulation Model
for Estimating Ground Level Concentrations
of Photochemical Pollutants

Philip M. Roth
Steven D. Reynolds
Philip J. W. Roberts

Report 71-SAI-17

June 1971

Prepared by

Systems Applications, Inc.
Beverly Hills, California 90212

for the

Air Pollution Control Office
of the Environmental Protection Agency
Durham, North Carolina 27701

under Contract CPA 70-148

ACKNOWLEDGMENTS

We are very grateful to Professor James G. Edinger of the Department of Meteorology at University of California at Los Angeles for his many contributions to this work. In addition to his direct participation in the preparation of surface wind maps, Professor Edinger gave readily of his time in a number of informative and helpful discussions.

We also wish to acknowledge the contributions of Clarence L. Nelson, William Tiedemann, and Vikram Budhraja to various aspects of this effort. Mr. Nelson supervised and coordinated all computer-related activities in the data preparation and digitization effort, including those associated with the interactive computer graphics system. William Tiedemann converted to digital form and entered onto coding sheets virtually all surface wind field data. Mr. Budhraja prepared and digitized all the maps of mixing depth. We wish to extend our thanks to each of these participants.

Finally, we wish to express our appreciation to the Shell Development Company, Emeryville, California, for permitting us to use their interactive computer graphics system. Dr. Richard W. Watson and Mr. Leonard Barton of their staff gave unstintingly of their time in rendering assistance to us.

CONTENTS

	Page
INTRODUCTION	C-1
I. THE INVERSION	C-4
A. The Inversion Over Los Angeles	C-6
B. The Work of J. G. Edinger	C-8
C. Vertical Temperature Profile Data	C-9
D. Preparation of Maps of Mixing Depth	C-17
E. An Evaluation	C-21
II. THE SURFACE WINDS	C-30
A. The Data	C-30
B. Preparation of Surface Wind Maps and Conversion to Digital Form	C-33
III. WINDS ALOFT	C-39
IV. TREATMENT OF TURBULENT DIFFUSIVITY	C-43
References	C-46

INTRODUCTION

Atmospheric transport and dispersion processes find expression in the overall airshed model in a number of ways, as can be seen from the governing conservation equations, in which horizontal turbulent diffusion is neglected:

$$\frac{\partial c_i}{\partial t} + u\frac{\partial c_i}{\partial x} + v\frac{\partial c_i}{\partial y} + w\frac{\partial c_i}{\partial z} = \frac{\partial}{\partial z}\left(K_z\frac{\partial c_i}{\partial z}\right) + R_i(c_1, c_2, \ldots, c_p) + S_i$$

$$i = 1,2,\ldots,p \qquad \text{(C-1)}$$

for
$$x_W \leq x \leq x_E$$
$$y_S \leq y \leq y_N$$
$$h(x,y) \leq z \leq H(x,y,t)$$
$$t \geq t_o$$

where
- x,y = horizontal coordinates
- z = vertical coordinate
- u,v,w = three components of average wind velocity vector
- c_i = time-averaged concentration of species i
- K_z = turbulent eddy diffusivity
- S_i = rate of emission of species i from elevated sources
- R_i = rate of production of species i through chemical reaction
- Y_W, Y_E, Y_S, Y_N = west, east, south, and north
- $h(x,y)$ = terrain elevation
- $H(x,y,t)$ = elevation of the inversion base above sea level

The initial and boundary conditions are:

initial
$$c_i(x,y,z,t_o) = f_i(x,y,z)$$

boundary (1)
$$-K_z\frac{\partial c_i}{\partial z} = Q_i(x,y,t) \qquad \text{at } z = h(x,y)$$

boundary (2) if $W \geq 0$, then $$-K_z \frac{\partial c_i}{\partial z} = 0$$

if $W < 0$, then $$W\, g_i(x,y,z,t) = W\, c_i - K_z \frac{\partial c_i}{\partial z} \qquad \text{at } z = H(x,y,t)$$

where $$W = w - u \frac{\partial H}{\partial x} - v \frac{\partial H}{\partial y} - \frac{\partial H}{\partial t}$$

(3) $$c_i = g_i(x,y,z,t) \qquad \text{at } x = x_W \text{ (or } x_E\text{)}$$
$$y = y_S \text{ (or } y_N\text{)}$$

where x and y are at boundaries through which the prevailing winds enter.

and where $Q_i(x,y,t)$ = surface flux of species i

$f_i(x,y,z)$ = initial concentration distribution of species i

$g_i(x,y,z,t)$ = function expressing the concentration of species i on the boundary at points of inflow.

Wind speed and *wind direction* enter through the component variables u, v, and w. The *height of the inversion base* H must be known in order to specify the boundary conditions, while the *turbulent diffusivity* K_z enters into both the continuity equations and the boundary conditions. One must look further, however, to appreciate the extent to which the incorporation of these meteorological variables dominates data preparation and model input requirements.

In order to integrate the equations of continuity using finite difference techniques, it is necessary to create a three-dimensional network of cells having nodes at their centers. In our case, this array is comprised of 625 nodes in each of ten horizontal layers up to the inversion, a total of 6250 nodes. The three components of the wind velocity vector must be specified at each node point for each time step. This may be accomplished in part by constructing maps which represent the surface wind field for hourly time intervals using data gathered at the network of ground-based monitoring stations. Unfortunately, virtually no measurements are made of the winds aloft. (Of particular interest is the wind field up to about 3000 feet above the ground.) This wind field must be specified, however, so as to satisfy the requirement of conservation of mass at the surface and aloft for both air and pollutant species. It is thus necessary either to construct or to calculate wind fields at regular time intervals for all horizontal layers between the ground and the base of the inversion. Finally, spatial and temporal variations in the height of the inversion base must also be entered as data--625 values of H for each hourly interval.

It is clear that a very large amount of meteorological information must be collected, codified, stored, and retrieved in order to carry out the necessary calculations. For example, thirteen hourly wind fields at the ground and thirteen hourly inversion maps are required to simulate a twelve-hour time period. This is the equivalent of nearly twenty-five thousand data entries (625 x 13 x 3)--and this despite the fact that the wind field aloft is not entered as data, but is generated by the computer program. We emphasize that these data constitute the input requirements for the daylight hours of *only one validation day.*

It is apparent that methods of generating, manipulating, and transferring meteorological data are needed that are more sophisticated than manual drafting and translation of hand-drawn maps to punched cards. The elimination of the manual preparation of maps would also be most welcome. Unfortunately, with the exception of two efforts that have yet to bear fruit (and which will be described)--the development of a model of inversion behavior and the application of computer graphics in the preparation and digitization of wind maps--we have not been able to give adequate attention to the problem, largely due to limitations in time. The development of methods and models for organizing, codifying, and transferring meteorological data, in fact, constitutes a task of highest priority in future work if the airshed model is to be of general applicability.

Having discussed the difficulties experienced in the treatment of meteorological variables, we turn now to achievements--the preparation and conversion to digital form of contour maps of surface wind speed and direction (isotachs and streamlines, respectively) and of the height of the inversion base--in each case hourly representations. We have also explored several approaches to the calculation of the wind field aloft, one of which appears to be a useful method for the automatic generation of these wind fields. The four sections that follow are concerned respectively with inversions, surface wind fields, winds aloft, and turbulent diffusivities. In each section we describe, for the days of validation,

1) the computational and data requirements,
2) the nature of the available data base,
3) our efforts in satisfying the stated requirements, and
4) the deficiencies in our approach and, thus, recommended future efforts as they relate to the particular aspect of meteorology under discussion.

I. THE INVERSION

A crude measure that is often invoked to characterize air pollution potential is the ventilation factor U(H-h), where U is the mean wind speed and H-h is the mean depth through which mixing occurs. When an inversion is present, H is the mean elevation of the inversion base. The ventilation factor decreases, and the potential for "smogginess" increases, if either U or H-h assumes a low value for any length of time. As knowledge of these variables is of major importance in the prediction of ground level concentrations, we must have the capability of incorporating these variables, and their variations in space and time, into our model. In this first section, we focus on the nature of the inversion that persists over the Los Angeles Basin during the summer and autumn months. In subsequent sections, we direct our attention to the wind field.

The degree to which pollutants will mix and disperse vertically is best characterized by considering the change in temperature of the ambient atmosphere with height, the negative of which is termed the lapse rate, Γ, where

$$\Gamma = -\frac{dT}{dz} \quad .$$

Typically, the lapse rate observed in the lowest levels of the atmosphere is positive, i.e., temperature decreases with height. To determine the extent to which vertical mixing and dispersion will occur in an atmosphere of known lapse rate, it is only necessary to compare that lapse rate with the adiabatic rate of cooling, Γ_o. (See Figure C-1). Γ_o is the rate of cooling a rising parcel of air will undergo when no heat is exchanged between the parcel and its surroundings. Suppose, for example, that a parcel of pollutant-bearing air is displaced upward in an atmosphere in which $\Gamma > \Gamma_o$. The rising parcel will expand adiabatically and its temperature will decrease, but at a less rapid rate than the decrease in atmospheric temperature with height. Thus, the parcel will be at a higher temperature than its surroundings, and being less dense than the surrounding air, will continue to rise. Similarly, displacement downward will result in continued sinking. Thus, an atmosphere in which $\Gamma > \Gamma_o$ is unstable relative to vertical displacements. High dispersion rates and low pollutant concentrations typify this atmospheric condition.

In contrast, the atmosphere is stable to vertical displacements when $\Gamma < \Gamma_o$. A parcel displaced upward will be cooler, and thus more dense, than its surroundings. It will thus tend to sink to its original vertical position. Downward displacements are also stable. Consider now atmospheric conditions under which Γ is negative, e.g., temperature increases with height. Such conditions, termed inversions, represent an extreme in atmospheric stability, conditions under which vertical displacements are almost entirely suppressed. Finally, we may wish to characterize the *strength* of an inversion, and thus the degree to which it will suppress vertical dispersion, by the magnitude of the quantity $\Gamma_o - \Gamma$. It is clear that the greater the slope of the vertical temperature profile $\frac{d\Gamma}{dz}$, the more stable is the inversion layer.

Figure C-1 follows.

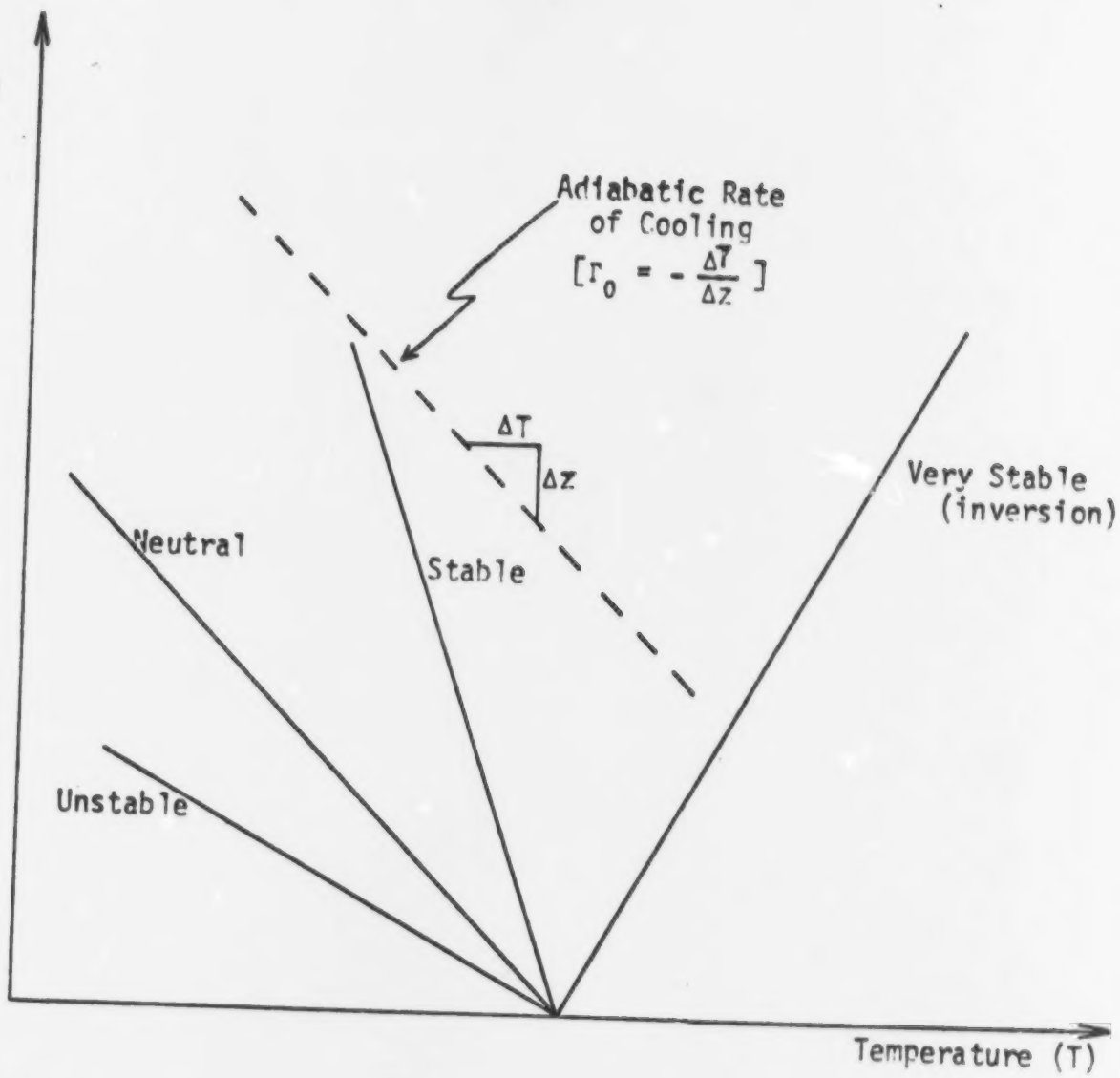

FIGURE C-1. Representative Atmospheric Temperature Profiles

Inversions form in one of two ways, through cooling from below or heating from above. Inversions often form, particularly at night, due to radiation cooling at the ground. Horizontal movement of an air mass from above a warm surface (land) to above a cool surface (water) also produces an inversion. (Note that at night the land surface may be cooler than the water). Such inversions are termed *ground-based* or *surface* inversions. Inversions that are the result of heating from above involve the spreading, sinking, and compression of an air mass as it moves horizontally. As upper layers undergo the greatest elevation change, they experience the greatest degree of compression and thus the greatest increase in temperature. If the temperature increase is sufficient, an inversion will result. The sinking and compression process is termed *subsidence* and is associated with the clockwise movement of air accompanying anticyclones.

The two types of inversions described, surface and subsidence, are over-simplified representations of the vertical temperature profiles that commonly occur over urban areas. More typical are the profiles shown in Figure C-2. Their most notable feature is that the lapse rate in the lowest layer is nearly always neutral or unstable. The persistence of this temperature profile during the night is due primarily to the release to the atmosphere of heat absorbed by buildings, streets, and other city surfaces during the day. The disturbance of flow and the promotion of mixing by buildings and other city structures also aids in establishing a mixing layer. Vertical mixing is suppressed, however, throughout the elevated inversion, denoted by the dashed line in each profile. Thus, though an inversion is present over a city, there is a region through which mixing is vigorous and which can be characterized by a "mixing height", the distance from the ground to the base of the inversion.

A. The Inversion Over Los Angeles

During the summer months the North Pacific anticyclone, a major high pressure area, maintains a virtually stationary position several hundred miles off the coast of California. Air emanating from this "high" moves in a southeasterly direction along the Pacific Coast. Subsidence occurs during this horizontal movement, heating the upper layers through adiabatic compression. The lower levels of this air mass are also heated, but to a lesser extent, during the course of the journey over water, moving from colder to warmer (near the coast) regions of the ocean. Mixing induced due to this warming process results in the entrainment of moisture and the establishment of the "marine layer", a layer several hundred feet deep. Finally, the air mass encounters cold subsurface waters that have welled-up at the coast. The lowest layers are cooled and, depending on the amount of water in the air, the air temperature, and the time of contact with the area of upwelling, fog may form. In any case, the cooling from below tends to form an inversion or strengthen an existing inversion.

Thus, air arriving over the Los Angeles Basin during the summer months undergoes a series of transport and energy transfer processes that tend to create an elevated inversion lying over a well-mixed marine layer. These processes occur over a spatial scale of the order of 1,000 miles. It is necessary to examine a much smaller scale, of the

Figure C-2 follows.

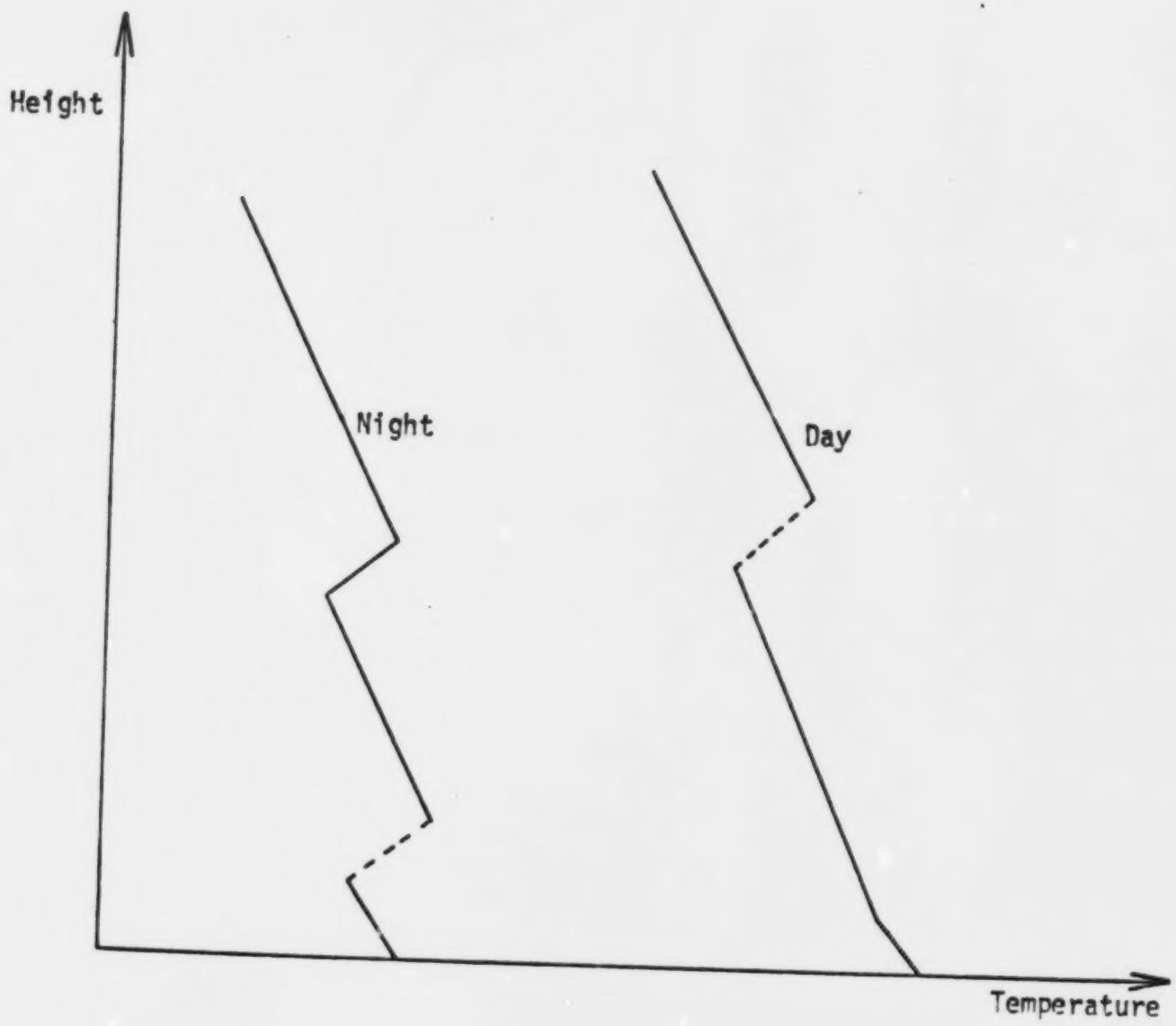

FIGURE C-2. Typical Vertical Temperature Profiles Above Cities (from Panofsky (1969))

order of 10 to 100 miles, to understand the behavior of the inversion over Los Angeles. Such an examination is necessary, because, unlike inversions of approximately constant depth that lie over urban areas situated inland, the depth of the well-mixed layer over Los Angeles varies substantially from place to place at any instant in time. For example, during the early afternoon it is not unusual for the height of the inversion base over terrain at the coast to be one-fourth the height of the inversion base at a point twenty miles inland. If the air were stagnant and pollutants were injected into the atmosphere at equal rates at both points, concentrations near the coast may reach levels four times greater than those at the inland location. It is thus necessary to have knowledge of both spatial and temporal variations in mixing depth in order to develop an accurate airshed model.

B. The Work of J. G. Edinger

During the summer of 1957, Professor J. G. Edinger of UCLA carried out an extensive measurement program to investigate variations in depth of the marine layer over the Los Angeles Basin. Edinger and another pilot/meteorologist flew 116 flights over a 45-day period, measuring vertical temperature profiles over seven sites during each flight--at El Monte, Fullerton, Compton, Torrance, Santa Monica, Van Nuys, and Glendale.* As a result of analyzing the data he collected, Edinger (1959) was able to make the following generalizations: "The marine layer over the Los Angeles coastal plain during the daylight hours (a) is shallow at the coast and deep inland, (b) increases in depth early in the day and then becomes progressively shallower during the afternoon, and (c) reaches its maximum depth first at the coastal stations and later at the inland stations."

Analysis of the data collected indicated that variations in the depth of the mixing layer as a function both of location and time could be explained in terms of three atmospheric phenomena: (a) convergence or divergence of the horizontal wind within the layer, (b) dilution of the marine layer from above by the mixing of air from within the elevated inversion layer with the marine air, and (c) advection of deeper or shallower layers of marine air into the area.* The convergence-divergence effect, attributable to the sinking of air moving from the sea to the land, manifests itself through a decrease in depth of the marine layer during the morning hours. Mixing of air within the inversion layer with marine air is attributable to the warming of the earth's surface by solar radiation, thus initiating convective mixing processes which penetrate the elevated inversion. Advection (horizontal flow) determines the length of time over which this convective process occurs, the time of residence of the air mass over land. By considering each of the three mechanisms separately, then combining them, Edinger was able to develop a semi-quantitative model of changes in the depth of the marine layer. We refer the interested reader to Edinger (1959) for a full discussion of his findings.

---

* See Edinger (1959) for details.

In a subsequent study Edinger and Helvey (1961) examined the structure of one of the two major zones of horizontal wind convergence that occur on the boundaries of the Los Angeles Basin--the San Fernando and Elsinore convergence zones (see Figure C-3). The region that he examined and the one of interest to us, because it falls within the bounds of our modeling area, is the San Fernando convergence. Using observational data, Edinger was able to construct a vertical wind pattern that results from the convergence of two air masses, explore the variations in location of the zone with time of day, and gain some insight into the redistribution of ground-based pollutants by the rising flow of air produced by the converging winds.

Edinger's work (the 1959 study, in particular) has provided the basis for the development of maps of the depth of the well-mixed layer as a function of horizontal spatial coordinates and time. In particular, we prepared maps showing the estimated average depth of the well-mixed layer over each of the 625 2 mile x 2 mile grid squares for each of the thirteen hours between 6 AM and 6 PM PDT for 29 and 30 September 1969. To do this, however, we required measurements of mixing depth on the two days of interest. In the two sections that follow we describe the pertinent data available for the two validation days, the rationale and procedures upon which the preparation of maps were based, and examples of the completed maps.

C. Vertical Temperature Profile Data

Generally speaking, the only vertical temperature soundings taken over the Los Angeles Basin prior to May 1971 were the radiosonde measurements made twice daily at Los Angeles International Airport (LAX)--at 6 AM and 10 AM PST. (Since May 1971 measurements have been made routinely at El Monte). During the summer of 1969, however, the Scott Research Laboratories, as part of a comprehensive data gathering program, flew 26 aircraft flights over the Los Angeles Basin in order to make measurements of chemical and meteorological variables in the atmosphere. Two flights were made on both 29 and 30 September, commencing at about 7:30 AM and noon PST each day. These flights originated and terminated at El Monte Airport and had a duration of approximately 1½ hours. The flight plan is illustrated in Figure C-4 and is described in detail in the Scott Research Laboratories report (1970, Vol. I, p. 3-2).

Essential to the determination of inversion height is the measurement of vertical temperature profiles during spiral ascents and descents. Such profiles were measured at the points 1, 2, and 5 in Figure C-4--at El Monte, Commerce, and Hawthorne respectively. The morning and mid-day profiles measured at these locations on 29 and 30 September 1969 are shown in Figures C-5 through C-7. (See Scott Research Laboratories (1970, Vol. IV) for a complete listing of the data.) The LAX radiosonde profiles for these days are given in Figure C-8. Corresponding depths of the well-mixed layer, as recorded in Table C-1, were determined from these profiles.

Figures C-3 to C-8
and Table C-1 follow.

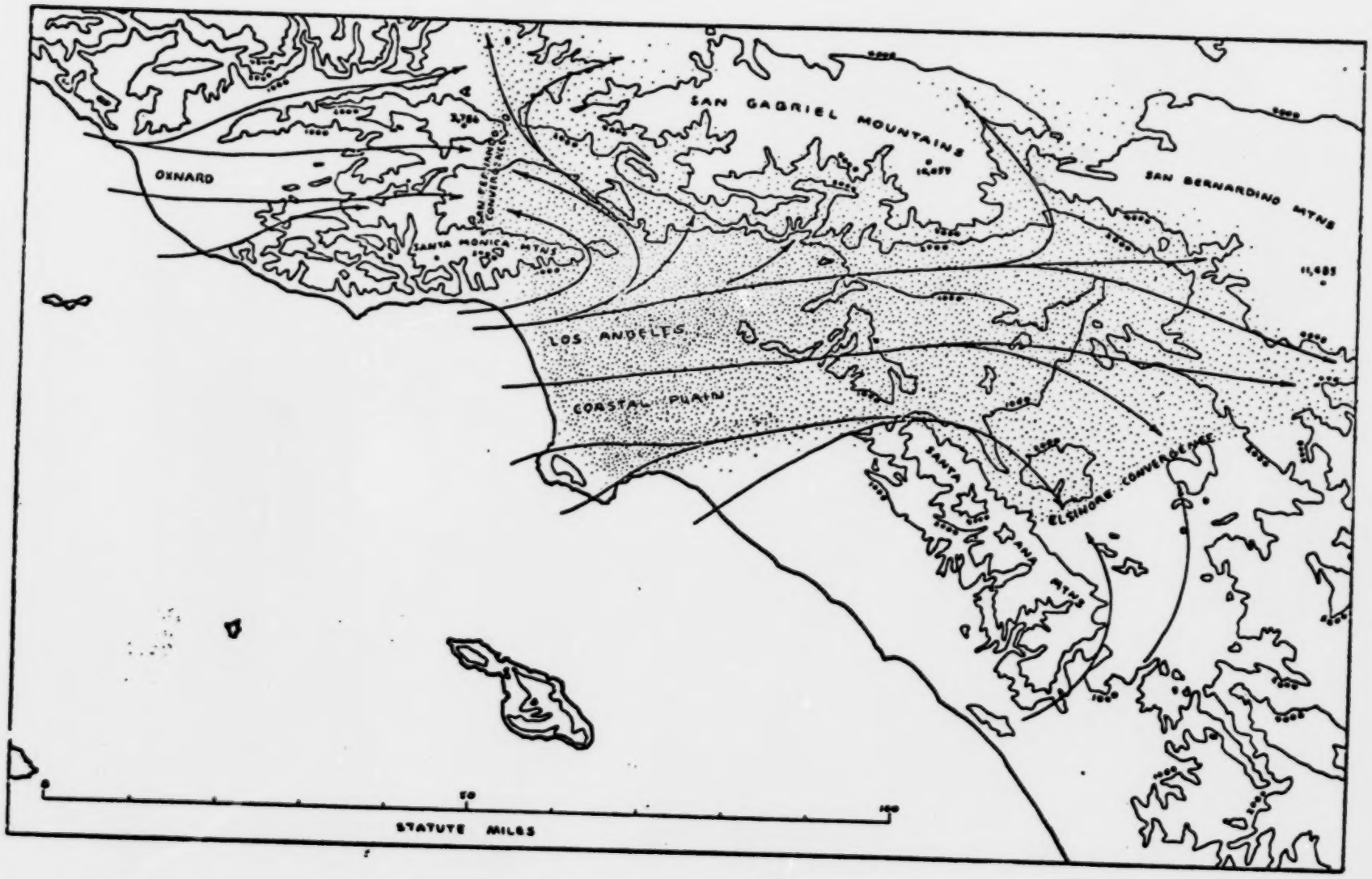

FIGURE C-3. Path of Pollutant Transport Over the Los Angeles Area During Typical Sea Breeze (from Edinger and Helvey (1961))

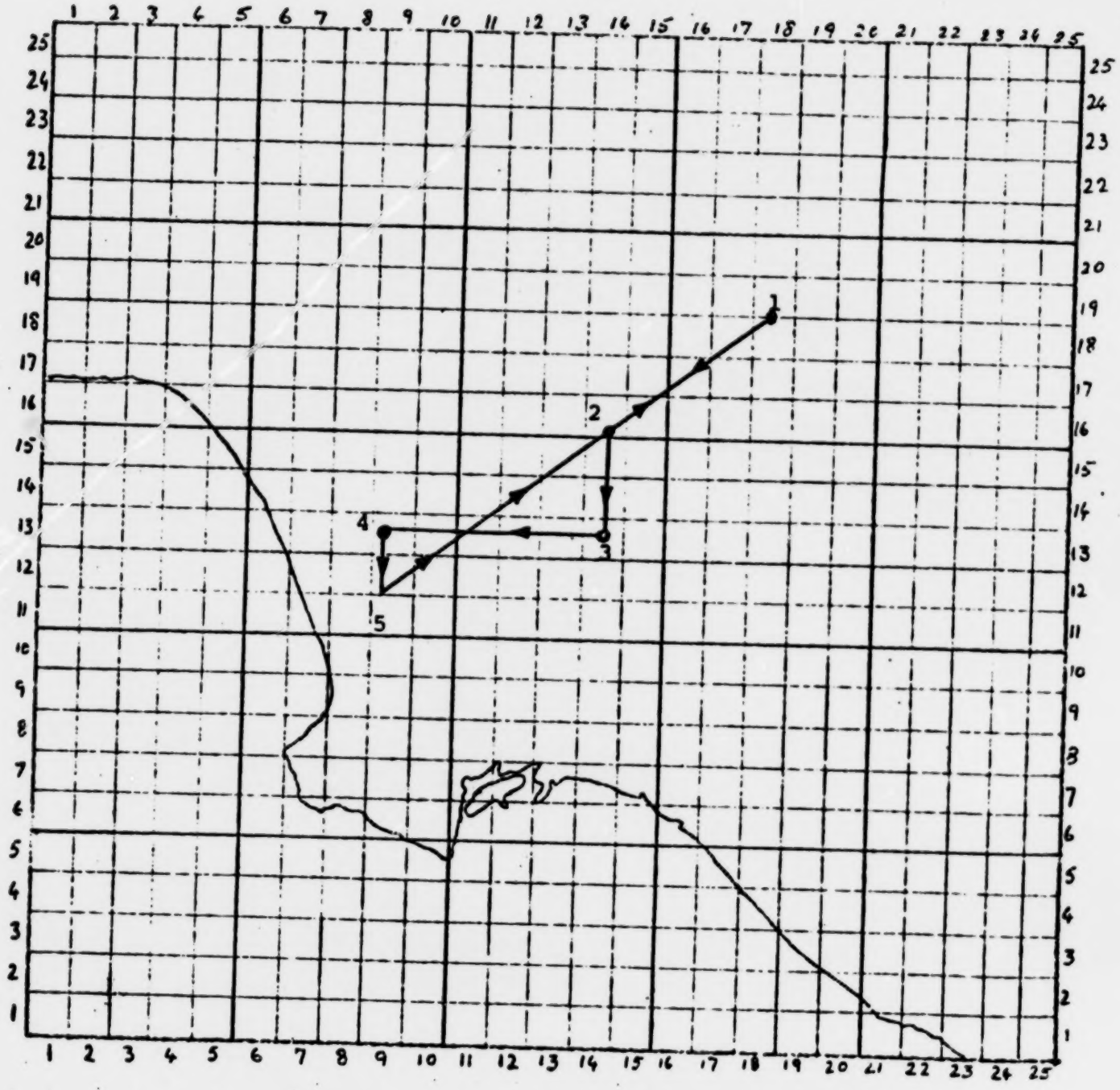

1. El Monte Airport
2. Commerce
3. Intersection of Los Angeles and Rio Hondo Rivers
4. Hawthorne Airport
5. Alondra Park

Spiral ascents and/or descents to collect data were made over El Monte, Commerce and Alondra Park.

Figure C-4. Aircraft Flight Plan

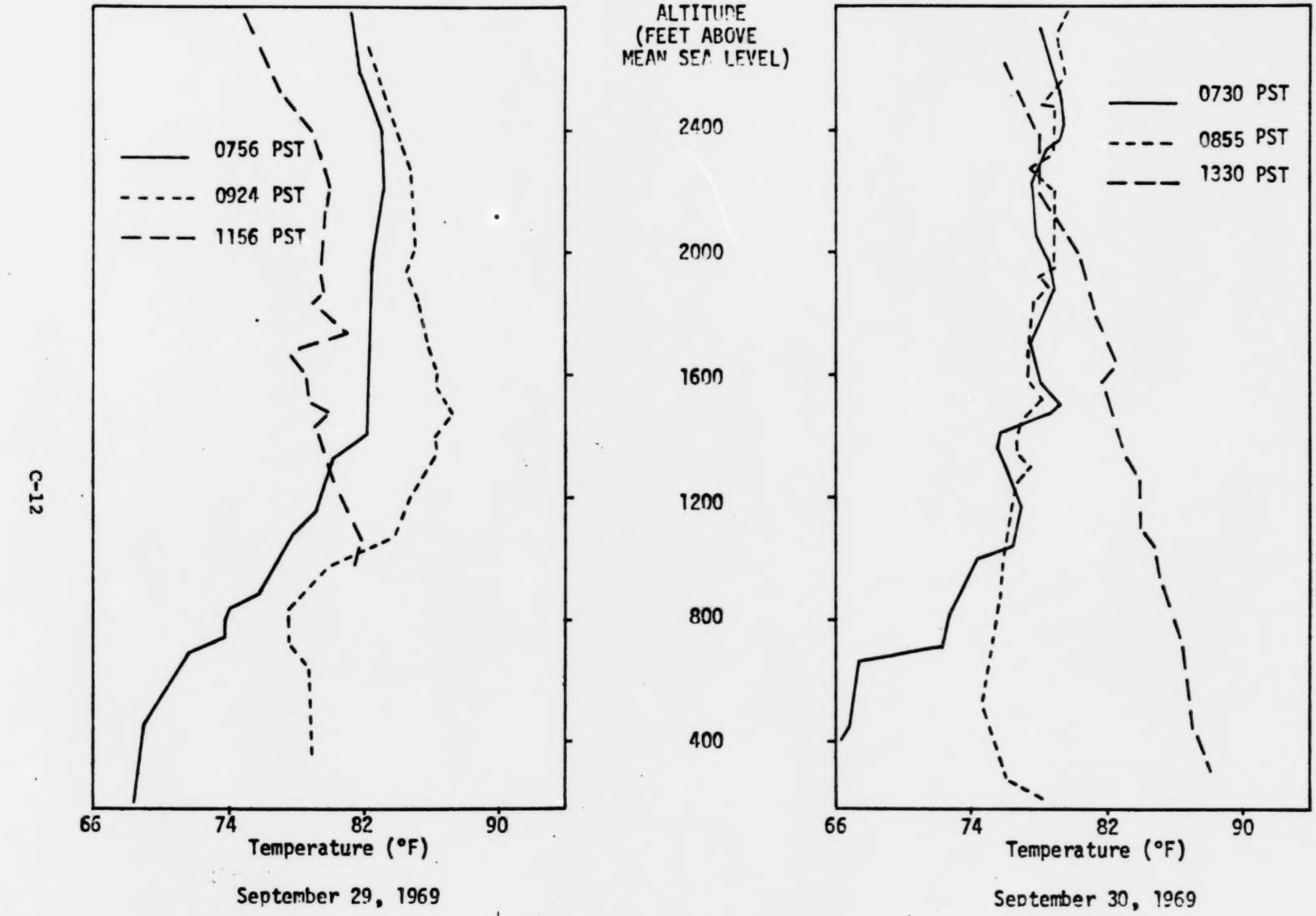

FIGURE C-5. Vertical Temperature Profiles Over El Monte

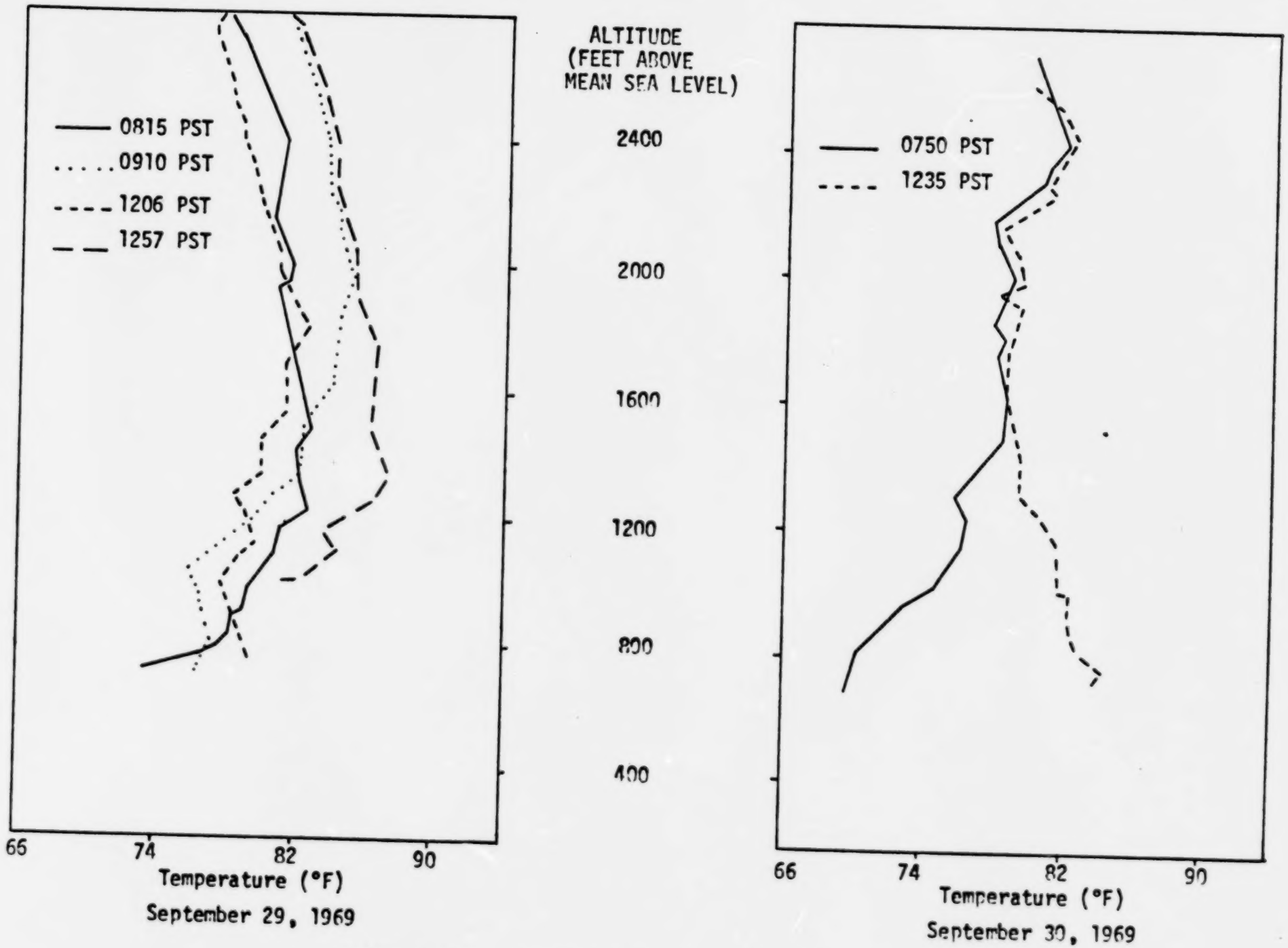

FIGURE C-6. Vertical Temperature Profiles Over Commerce

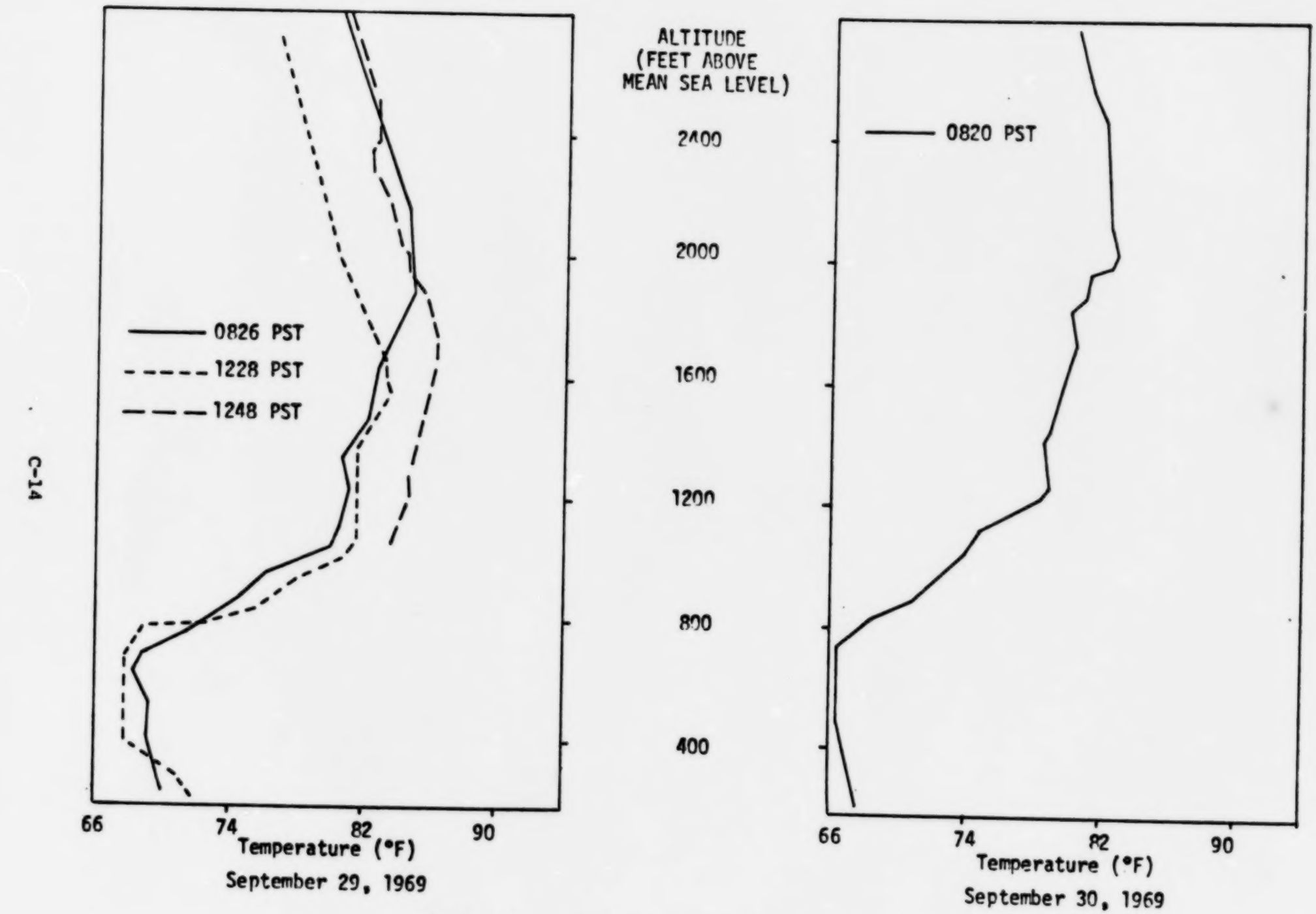

FIGURE C-7. Vertical Temperature Profiles Over Hawthorne

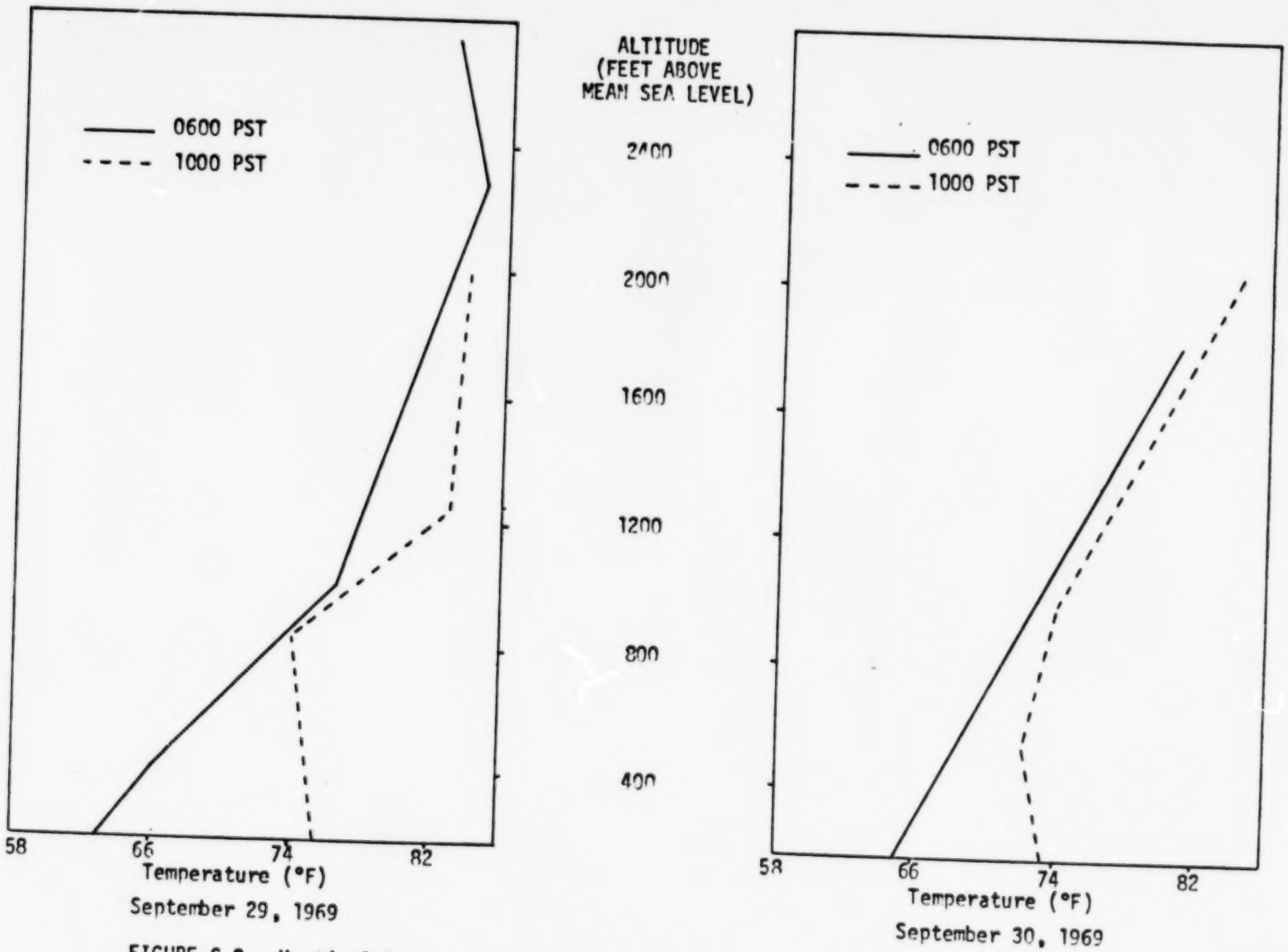

FIGURE C-8. Vertical Temperature Profiles Over Los Angeles International Airport

TABLE C-1. Height of The Inversion Base, As Taken From Vertical Temperature Soundings over Four Locations in the Los Angeles Basin

Location	29 September 1969		30 September 1969	
	Time (PST)	Height of the Inversion Base, H (feet above mean sea level)	Time (PST)	Height of the Inversion Base, H (feet above mean sea level)
Commerce	0815 0910 1206 1257	600 850 1300 1000	0750 1235	800 1700
El Monte	0756 0924 1156 1312	450 825 1700 a	0730 0855 1330	500 800 2900
Hawthorne	0826 1228	650 700	0820	740
Los Angeles International Airport	0600 1000	550 750	0600 1000	500 540

a) Inversion breaks up; a height of 2800 feet assigned.

D. Preparation of Maps of Mixing Depth

Measured vertical temperature profiles, along with the guidelines based on the findings of Edinger and other investigators, formed the strategic basis for the preparation of maps of mixing depth. We consider first the procedures by which mixing depth contours for the Los Angeles Basin were constructed. (Rules applicable to ocean and mountain regions and the San Fernando Valley will then be discussed.) One of the observations made by Edinger is that contours of the inversion base over the Los Angeles Basin (that portion of the modeling region south of the Santa Monica Mountains) roughly parallel the curvature of the local coastline. The three points at which aircraft soundings were made, 1, 2, and 5 in Figure C-4, all lie within the Basin and are colinear, with separations of 12½ miles and 10 miles between points 5 and 2 and between points 2 and 1, respectively. Furthermore, the line connecting 5 and 1 is approximately perpendicular to the coastline. We thus adopted the following strategy:

a) Interpolate in time between the 8 AM and 1 PM soundings at each of the three measurement sites to estimate average hourly heights of the inversion base at these sites. (LAX and Hawthorne are separated by only 2½ miles and are approximately equidistant from the coast. They are thus considered as having about the same mixing depth). Extrapolate prior to 8 AM and after 1 PM. Interpolation and extrapolation rules may be inferred from observed variations in mean height of the inversion base and observed variations of these height/time profiles with distance from the coast (see Edinger (1959) for details of variational patterns). See Tables C-2 and C-3 for interpolated and extrapolated values.

b) In accordance with Edinger's findings, plot contours of constant height of the inversion base on hourly maps (6 AM - 6 PM PDT), the contours being roughly parallel to the coastline. Enter at the three colinear sites on each of the thirteen maps the mean height of the inversion base, as estimated in (a).

c) For each map, interpolate in space along the line connecting Hawthorne (point 5) and El Monte (point 1). As the line is approximately perpendicular to the contours, average heights of the inversion base assignable to each contour can be estimated through this procedure. (As an example, see Figure C-10).

In this way, the height of the inversion base may be estimated throughout the Los Angeles Basin during the daylight hours.

This procedure, unfortunately, may only be used for the Basin; other rules are needed to estimate variations in the height of the inversion base over the San Fernando Valley and over mountainous areas. Thus:

Tables C-2 and C-3 follow

TABLE C-2. Height of The Inversion Base
Over Three Colinear Locations in the Los Angeles Basin
Interpolated and Extrapolated Values for September 29, 1969

Time (PST)	Location		
	Hawthorne	Commerce	El Monte
0600	500	360	375
0700	525	400	450
0800	550	460	500
0900	650	800	700
1000	750	950	950
1100	725	1100	1300
1200	700	1250	1650
1300	700	1000	2800
1400	700	950	
1500	675	900	Inversion breaks up
1600	650	800	
1700	650	750	
1800	650	750	

TABLE C-3. Height of the Inversion Base
Over Three Colinear Locations in The Los Angeles Basin
Interpolated and Extrapolated Values for September 30, 1969

Time (PST)	Location		
	Hawthorne	Commerce	El Monte
0600	500	550	350
0700	550	600	400
0800	600	750	500
0900	700	800	800
1000	650	1150	1300
1100	600	1500	1900
1200	550	1700	2500
1300	550	1600	2900
1400	550	1500	2600
1500	550	1200	2300
1600	550	1000	1900
1700	450	900	1400
1800	450	700	1050

d) For the San Fernando Valley, the assigned mixing depth (height of inversion base less terrain height) is equal to that over El Monte at the same time. This rule was adopted as the residence time over land of air over the Valley, and thus the time available for convective heating of the air, is about equal to that of air over El Monte during the daylight hours. As a result, the lapse rate profiles are expected to be similar at both locations.

e) The contour surface representing the height of the inversion base will be allowed to intersect the terrain for mountain areas adjacent to the ocean. (Actually, this rule was later ignored so as to avoid zero mixing depths). Inland, however, a mixing depth of 50 feet is assumed for the early morning hours, increasing thereafter. In accordance with observations made in other regions, the maximum allowable mixing depth over mountains is 600 feet.

Finally, the following general rules were adopted:

f) In the absence of specific data and at points removed from regions where interpolation is reliable, it was assumed that mixing depth increases during the morning hours (after sunrise) at a rate of about 200 feet per hour in the absence of advection (an increase of about 300 feet per hour due to surface heating and a decrease of 100 feet per hour due to convergence-divergence effects. See Edinger (1959) for details). In the presence of advection, the rate of rise was assumed to be the sum of (a) a surface heating effect--a rise of 300 feet per hour times the time (in hours) of residence of the air parcel over land and (b) a convergence-divergence effect--a sinking of 100 feet per hour from 8 AM to noon, or a maximum decrease in height of 400 feet.

g) Subsequent to interpolation, certain checks were made:

1. Time at which peak height occurs is checked with Edinger's observations.

2. Variations in height of the inversion base with time, at any location, should correspond with contours reported by Edinger.

h) Contour lines follow the coast line (approximately) during the morning hours, but the pattern changes progressively through the day due to the effect of the wind (see Edinger (1959)).

i) If the inversion breaks up during the afternoon, (as it does for example, over El Monte, and probably over the San Fernando Valley also, on 29 September) the only mechanism working to restore it is refreshment of the sea breeze. A mixing height of 3000 feet was assigned to those regions over which the

inversion did break up, an exception being the high mountain region north and east of El Monte, where a height of 5000 feet was assigned.

j) Linear interpolation was used to arrive at magnitudes of mixing depths at locations between measurement points.

k) Minor changes in terrain height were ignored in the preparation of maps.

Upon completion of maps constructed according to these rules, a final step is necessary.

l) Smooth maps of mixing depth, $H(x,y,t) - h(x,y)$, then reconstruct $H(x,y,t)$. (A map of average ground elevations is given in Figure C-9). Nearly all previous steps in the procedure are based only on the estimation of $H(x,y,t)$, since both Edinger's model and collected data are reported for this variable (i.e., relative to sea level).

By following these rules, a map such as that shown in Figure C-10 can be extended to the entire modeling region and then converted to digital form by assigning values of mixing depth to each of the 625 2 mile x 2 mile grid squares, as shown in Figure C-13. The procedure outlined above was used to construct thirteen hourly maps for each of the two validation days. Figures C-10 to C-12, along with Figures C-13 to C-15, illustrate the variations that occur throughout the morning and mid-day hours of one of the validation days.

E. An Evaluation

The procedure for estimating mixing depths that we have outlined is based on a very limited amount of data (three or four soundings taken twice a day) and on a semi-quantitative model derived from a comprehensive measurement program. The accuracy of the procedure is probably quite adequate for those regions for which heights of the inversion base were derived through interpolation. Inversion heights for the period before 8 AM and after 2 PM PDT and for the San Fernando Valley and mountain and ocean regions are certainly less accurate. The accuracy of these maps, however, probably compares quite favorably with the accuracy of the estimated wind fields (see Sections II and III).

The major problem that is faced in the construction of the maps is that a substantial amount of labor is involved in manual preparation and conversion to digital form. Approximately twenty man-days were required to carry out all steps in the process of converting original temperature profile data to maps of mixing depths, and these mixing depths to punched cards for input to the computer. If the airshed model is to be easily used, an automated procedure for the generation of mixing depths is mandatory.

Edinger's work offers a valid basis from which to develop an automated procedure. His model can be expressed quantitatively as:

Figures C-9 to C-15
follow

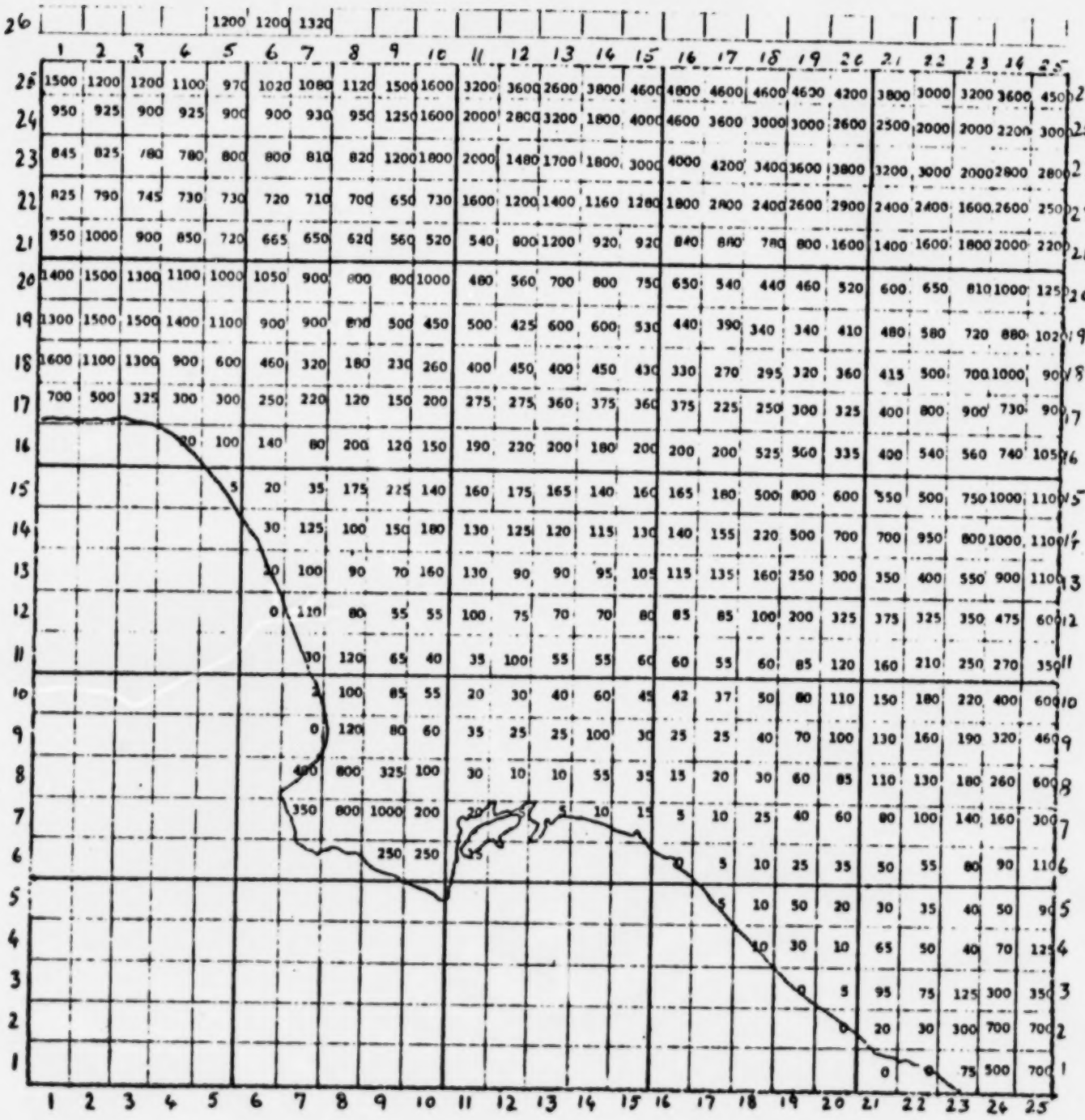

FIGURE C-9. Average Ground Elevations, h (feet)

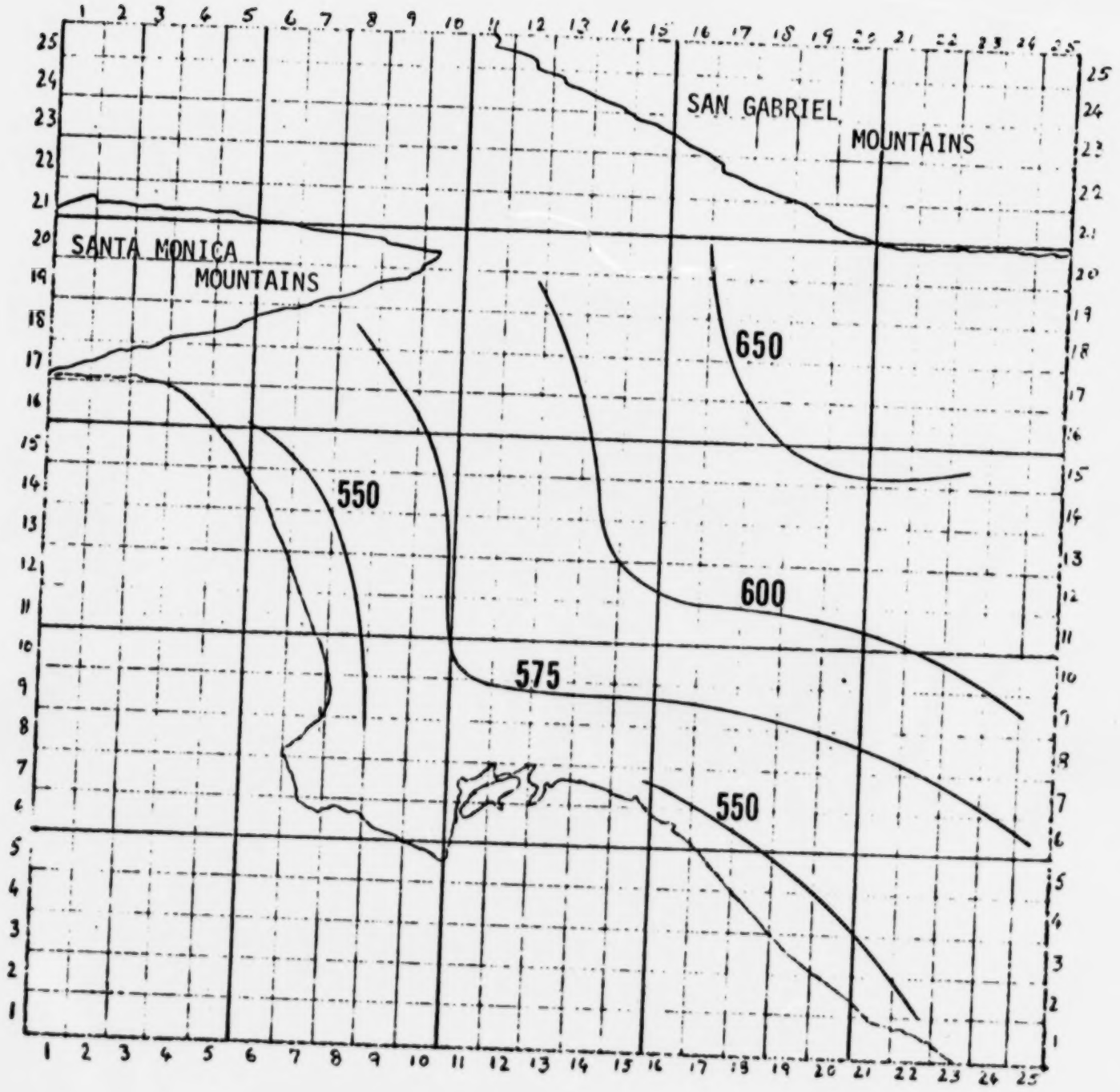

FIGURE C-10. Contours of the Height of the Inversion Base, H
Over the Los Angeles Basin at 7 AM PST on 29 September 1969
(Feet Above Mean Sea Level)

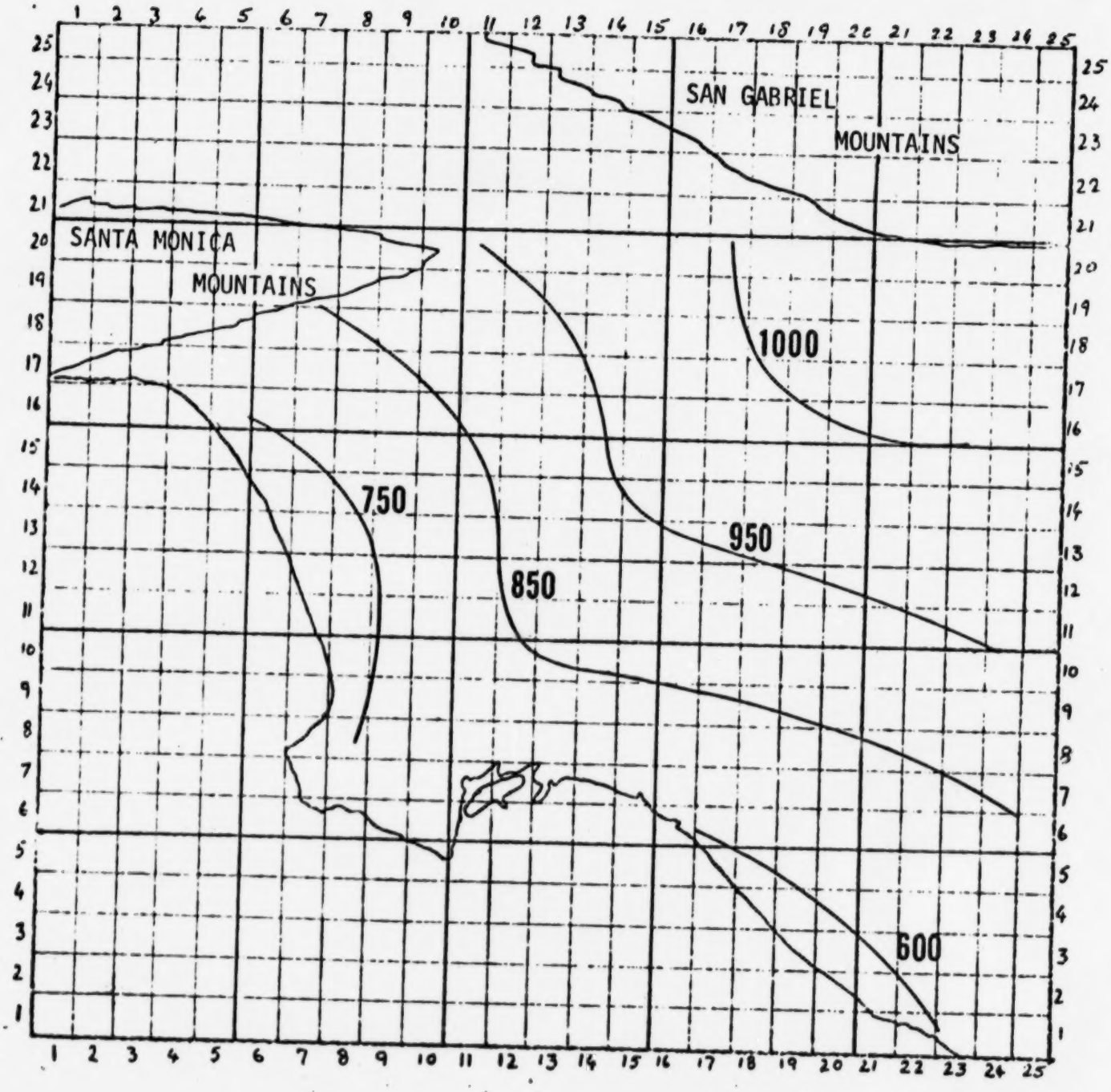

FIGURE C-11. Contours of the Height of the Inversion Base, H
Over the Los Angeles Basin at 10 AM PST on 29 September 1969
(Feet Above Mean Sea Level)

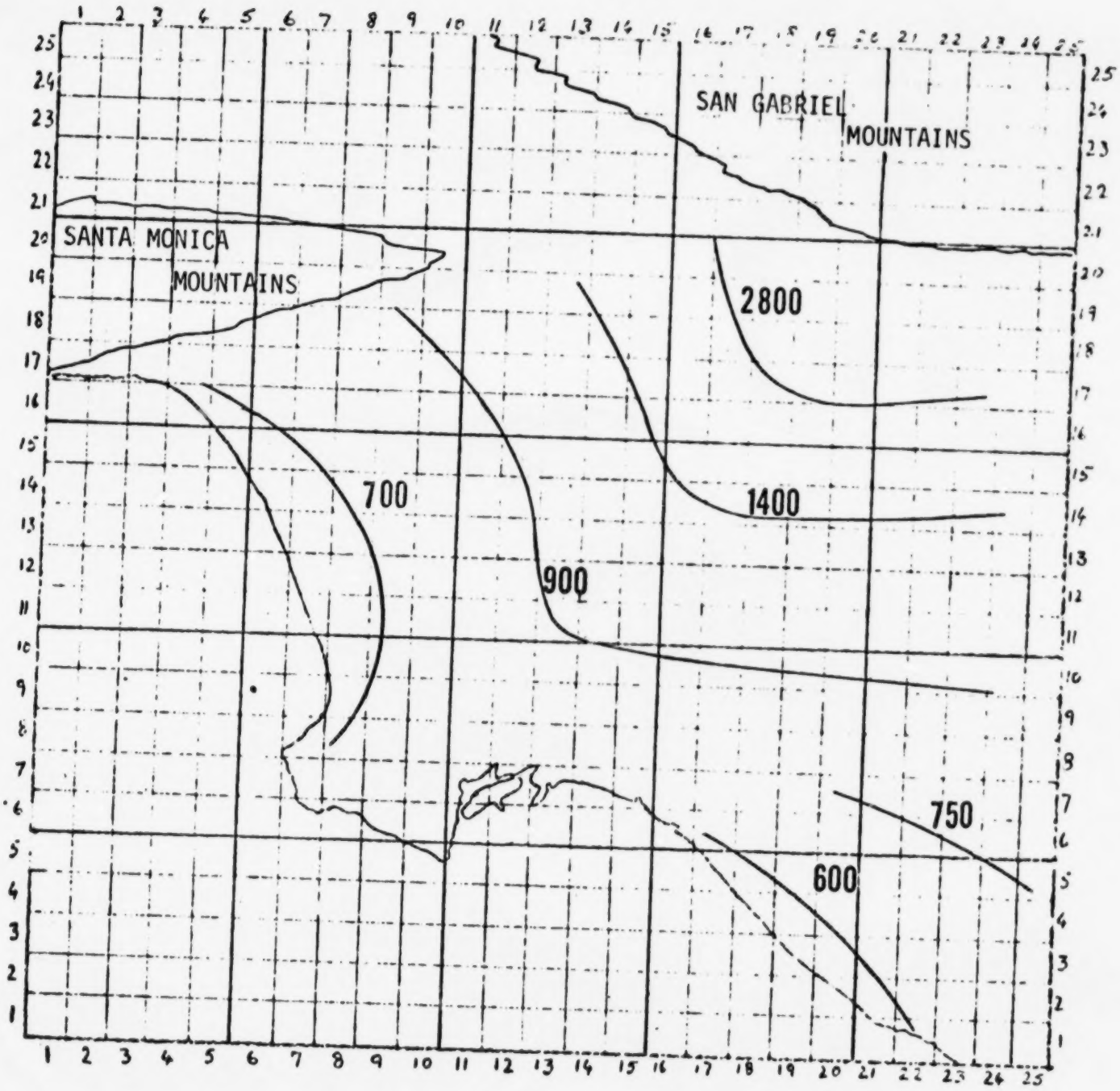

FIGURE C-12. Contours of the Height of the Inversion Base, H
Over the Los Angeles Basin at 1 PM PST on 29 September 1969
(Feet Above Mean Sea Level)

	1	2	3	4	5	6	7	8	9	10	11	12	13	14	15	16	17	18	19	20	21	22	23	24	25	
25	200	200	200	200	200	200	200	200	200	200	200	200	200	200	200	200	200	200	200	200	200	200	200	200	200	25
24	125	125	125	125	125	125	125	175	150	175	200	200	200	200	200	200	200	200	200	200	200	200	200	200	200	24
23	105	100	100	100	100	100	100	100	125	150	200	200	200	200	200	200	200	200	200	200	200	200	200	200	200	23
22	100	200	105	100	100	100	100	100	125	125	150	150	150	190	200	200	200	200	200	200	200	200	200	200	200	22
21	150	150	150	150	150	150	150	150	150	150	125	125	125	150	150	150	150	150	150	150	150	200	200	200	200	21
20	200	200	200	200	200	200	175	175	175	175	150	150	150	125	125	125	125	125	125	125	125	150	190	200	200	20
19	250	250	250	250	250	250	250	250	250	250	225	200	200	175	150	150	125	125	125	125	125	150	150	150	180	19
18	350	350	350	350	350	300	275	275	275	250	250	225	200	175	175	160	150	150	150	125	125	150	200	200	200	18
17	450	450	450	450	400	350	325	325	300	275	250	250	225	200	200	175	175	175	175	150	150	150	200	200	200	17
16	500	500	500	500	450	400	375	350	325	300	275	275	250	230	225	200	200	200	200	175	175	175	200	200	200	16
15	500	500	500	500	495	470	425	375	350	325	300	300	275	260	250	225	225	225	225	200	200	175	150	150	200	15
14	500	500	500	500	500	480	450	400	375	350	325	325	300	290	275	250	250	250	240	225	225	200	175	175	150	14
13	500	500	500	500	500	480	470	425	400	400	375	350	325	320	300	275	275	275	270	250	250	225	200	175	175	13
12	500	500	500	500	500	500	500	450	450	425	375	375	350	330	325	300	300	300	290	275	275	250	225	200	175	12
11	500	500	500	500	500	500	490	480	450	420	400	375	375	360	350	330	325	325	320	300	300	275	250	225	200	11
10	500	500	500	500	500	500	495	480	460	430	420	410	400	380	375	360	350	350	340	325	325	300	275	250	225	10
9	500	500	500	500	500	500	500	480	460	440	440	440	440	420	400	390	375	375	370	350	350	325	300	275	250	9
8	500	500	500	500	500	500	450	400	400	450	450	480	480	470	430	420	400	400	400	375	375	350	325	300	275	8
7	500	500	500	500	500	500	450	400	400	400	500	495	495	490	470	460	430	425	420	400	400	375	350	325	300	7
6	500	500	500	500	500	500	500	500	400	350	485	500	500	500	500	500	470	450	440	425	425	400	375	350	325	6
5	500	500	500	500	500	500	500	500	500	500	500	500	500	500	500	500	495	470	460	450	450	430	400	375	350	5
4	500	500	500	500	500	500	500	500	500	500	500	500	500	500	500	500	500	490	480	470	460	440	420	400	380	4
3	500	500	500	500	500	500	500	500	500	500	500	500	500	500	500	500	500	500	500	495	470	460	440	420	400	3
2	500	500	500	500	500	500	500	500	500	500	500	500	500	500	500	500	500	500	500	500	480	470	450	400	400	2
1	500	500	500	500	500	500	500	500	500	500	500	500	500	500	500	500	500	500	500	500	500	500	470	400	350	1
	1	2	3	4	5	6	7	8	9	10	11	12	13	14	15	16	17	18	19	20	21	22	23	24	25	

FIGURE C-13. Estimated Mixing Depths, H-h, Over the Los Angeles Basin At 7 AM PST on 29 September 1969 (feet)

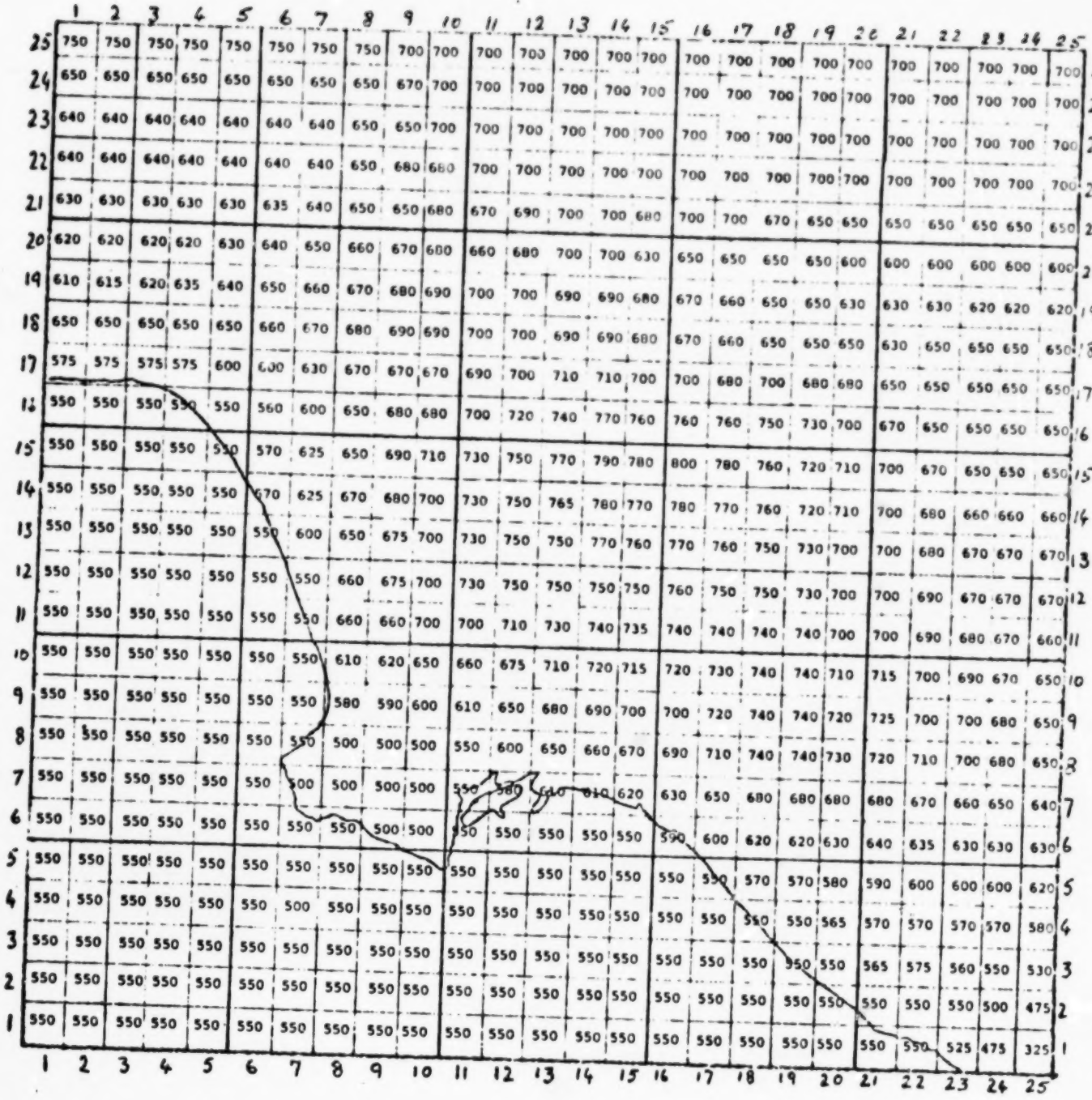

FIGURE C-14. Estimated Mixing Depths, H-h, Over the Los Angeles Basin At 10 AM PST on 29 September 1969 (feet)

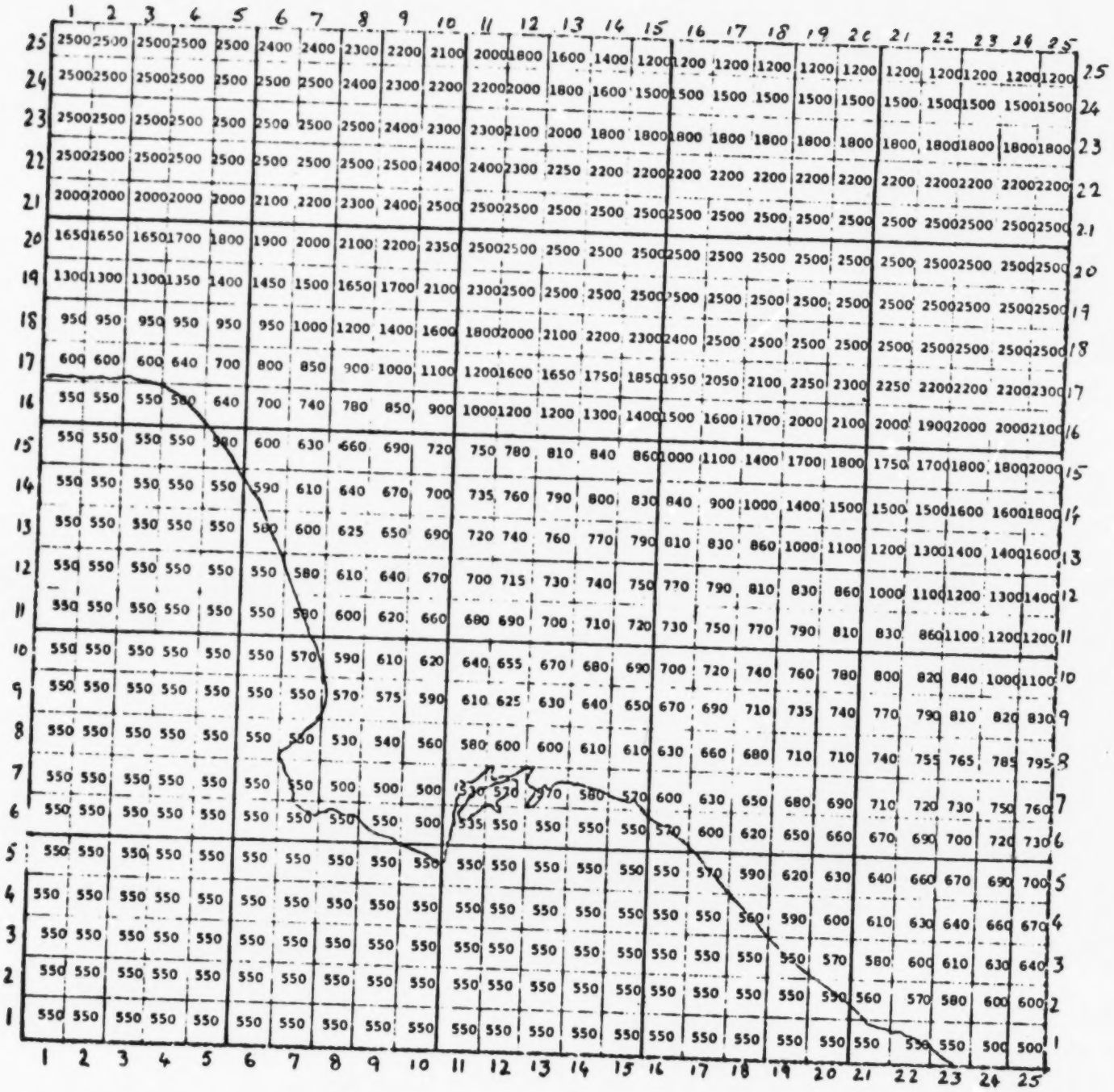

FIGURE C-15. Estimated Mixing Depths, H-h, Over the Los Angeles Basin At 1 PM PST on 29 September 1969 (feet)

$$H(x,y,t) = H^{o}(x,y) - 100\ (t-8) + 300r(x,y)$$

for $8 \leq t \leq 12$ (noon)

$$= H^{o}(x,y) - 400 + 300r(x,y)$$

for 12 (noon) $\leq t \leq 16$

and $H(x,y,t) > h(x,y)$ for all t

where $H(x,y,t)$ = height of the inversion base (feet)
$h(x,y)$ = elevation of terrain (feet)
t = time (in hours PST)
$r(x,y)$ = time that a parcel of air at (x,y) has spent over land
$H^{o}(x,y)$ = initial height of the inversion base (i.e., at t = 8)

We applied this model, in conjunction with the wind maps of Section II (needed to determine r), in the prediction of inversion height at the points at which vertical soundings were taken on the two validation days (i.e., the data were *not* included as a part of the calculation, but only as a standard of comparison). The computed values of H(x,y,t) compared favorably with experimental values (± 100 ft.) for each of the three measurement sites for the morning hours. However, comparisons were poor (with some exceptions) for the noon and early afternoon hours. While we were able to identify some of the reasons for the afternoon discrepancies, time did not permit the pursuance of this predictive effort. We believe, however, that a model of this type can be developed for the prediction of inversion heights over the Los Angeles Basin, and that an attempt should be made to do so.

While this approach to the development of a prediction model requires a relatively short time to develop, other, more theoretically sound approaches might also be considered. The solution of the boundary layer equations for coupled energy and momentum transport, although potentially very difficult problems, may prove to be a useful approach. Or, more simply, the solution of the energy equations, in conjunction with a constructed wind field (as described in the next section) might be considered. However, regardless of the modeling approach adopted, it would also be most useful if

1) Measurements of inversion height were made during the summer in portions of the modeling area and at times not included in or covered by the Edinger study.

2) *Routine* measurement of vertical temperature profiles were made, not only at Los Angeles International Airport and El Monte, but at other sites in the modeling region as well.

II. THE SURFACE WINDS

As indicated earlier, the North Pacific anticyclone exerts the dominant influence over air movements along the Southern California Coast during the summer and autumn months. In general, daytime winds over Los Angeles move from the ocean to the land in an easterly direction with an average speed of about five to seven miles per hour (see Figure C-3). At night, there is a reversal in the direction of flow, and winds are typically light. The movement of air near the ground is heavily influenced, however, by the hills and mountains that surround the Basin--notably the Santa Monica, San Gabriel, and Santa Ana Mountains, and the Palos Verdes and Puente Hills. The effects of these terrain features--in channeling and re-routing flows, in inducing flow up inclined, heated surfaces during the day and down along these same, cooled surfaces during the night, and in creating regions of convergence and divergence--are paramount in determining the complex flow patterns that characterize air movements in the Basin. The heating (or cooling) that an air mass undergoes in flowing from sea to land (or from land to sea) also influences flow patterns, as do the unique roughness features of the city. While many studies have been carried out in an attempt to better understand the movements of air masses in the Basin (see, for example, Neiburger and Edinger (1954), Neiburger, Renzetti, and Tice (1956), and Bell (1959)), it remains virtually impossible to predict local surface wind behavior.

In the absence of a predictive capability,* we constructed manually a series of hourly surface wind maps describing the flow patterns in the Basin for the two validation days. These maps, converted to digital form, were the surface wind inputs to the airshed model. In this section we describe the meteorological data upon which the maps were based, the preparation of the maps, and their conversion to digital form. We also discuss briefly the need for automating these processes.

A. The Data

Surface wind speed and direction measurements were obtained from three agencies that routinely collect these data in the Basin--the Los Angeles County Air Pollution Control District (LACAPCD), the Orange County Air Pollution Control District (OCAPCD), and the Weather Bureau (WB) (since October 1970, the National Weather Service). In addition, Scott Research Laboratories made surface wind measurements at El Monte and Commerce during the validation period. The thirty-four measuring sites are shown in Figure C-16 and listed according to agency in Table C-4. Unfortunately, frequency of measurement and averaging period vary. Wind speed and direction averages are reported for periods of one hour, ten minutes, and one minute, depending on the particular measurement station. Averaging periods for each station are indicated in Table C-4.

---

*The solution of the momentum (or Navier-Stokes) equations is, in itself, more complex than the solution of the coupled Equations (C-1), and thus was not considered.

Figure C-16 and
Table C-4 follow

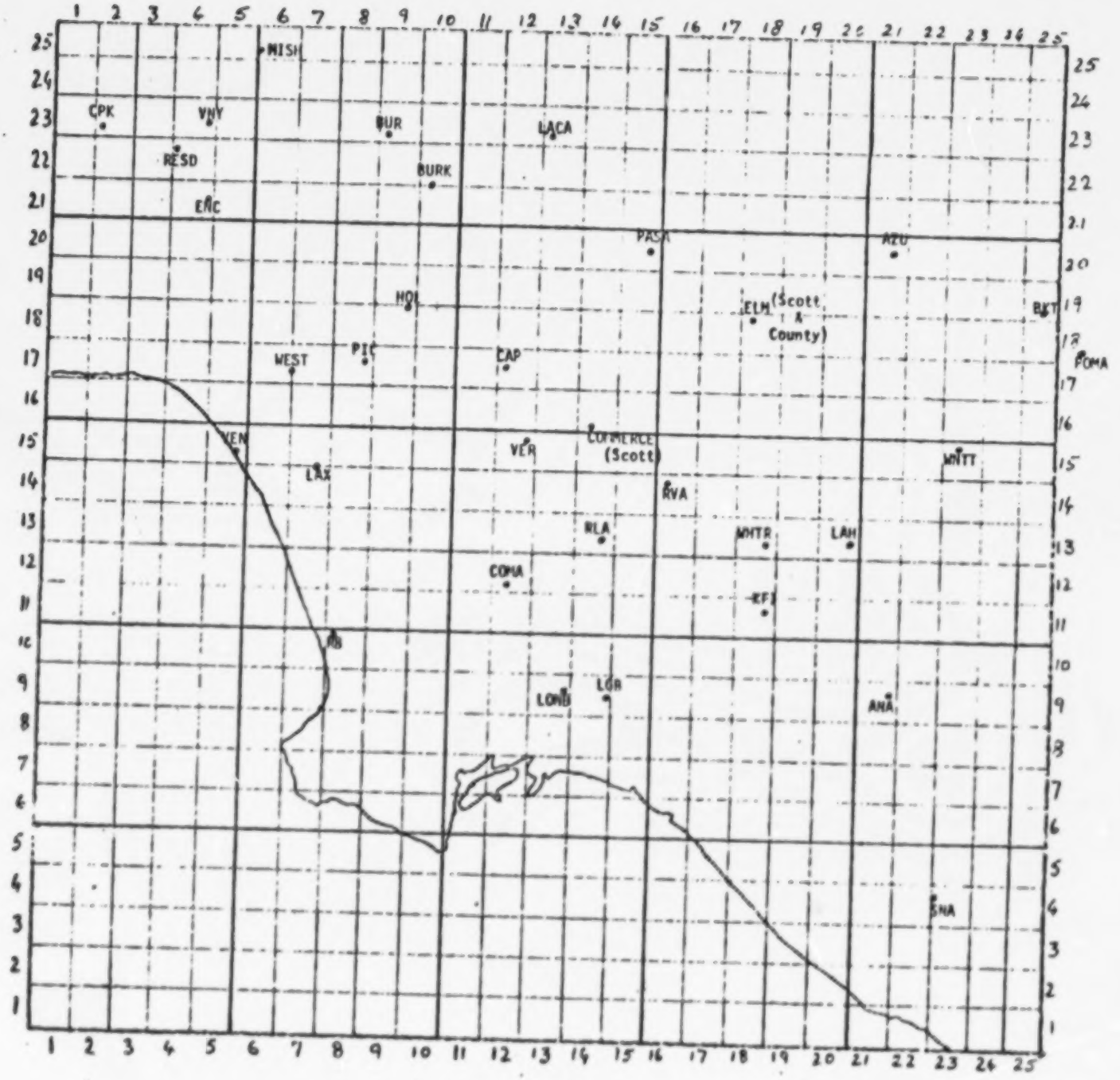

FIGURE C-16. Locations of Wind Measurement Stations Operative in the Los Angeles Basin in September 1969

TABLE C-4. Wind Measurement Status--Operating Agencies and Methods of Reporting Data

Los Angeles County
Air Pollution Control District

RB	(1)
VEN	(1)
RLA	(2)
PIC	(2)
HOL	(2)
VER	(2)
CPK	(1)
CAP	(3)
RVA	(1)
ENC	(1)
BKT	(1)
AZU	(1)
BURK	(1)
LONB	(1)
WEST	(1)
WNTT	(1)
RESD	(1)
LACA	(1)
POMA	(1)
ELM	(1)
COMA	(1)
MISH	(1)
WHTR	(1)
PASA	(1)
KFI	(1)
	25

Orange County
Air Pollution Control District

ANA	(3)
SNA	(3)
LAH	(3)
	3

Weather Bureau

LAX	(2)
LGB	(2)
BUR	(2)
VNY	(2)
	4

Scott

Commerce	(4)
ELM	(4)
	2

(1) Averaged over 1 hour between 1/2 hours, e.g. 6:00 = 5:30 - 6:30
(2) Instantaneous - averaged over 1 minute
(3) Averaged over 1 hour between hours, e.g. 6:00 = 6:00 - 7:00
(4) Ten-minute averages

In general, the measurement apparatus for both wind speed and direction have thresholds of approximately three miles per hour. Thus, these quantities are poorly determined during periods of low winds, which occur primarily during the night and early morning hours.

B. Preparation of Surface Wind Maps and Conversion to Digital Form

Initially, we considered two possibilities--manual preparation of surface wind maps and development of an interpolation scheme with which wind speed and direction would be computed automatically, given an array of measurements for the day in question. The obvious advantages of an interpolation scheme, when compared with manual procedures, were ease of use and savings in time. However, as we were concerned with only two validation days in this phase of development, we felt that it would be beneficial to prepare hourly representations of the wind fields--to get a "feel" for the data. The magnitudes of pollutant concentrations predicted using the airshed model were expected to be quite sensitive to the magnitude and direction of the wind vector, and we wished, not only to minimize inaccuracies, but also to be aware of the sources of inaccuracies. Thus, while realizing the need for an automated computational procedure, we postponed its development.

At the outset, we realized that the assistance of a person having an intimate knowledge of Los Angeles' unique meteorology was mandatory. We approached Professor Edinger and asked if he would aid in the preparation of the maps. He consented, and, in fact, prepared the full set of maps for both validation days. We supplied Professor Edinger with thirteen hourly maps for each day (6 AM to 6 PM PDT), with wind speed and direction indicated on each map at each of the thirty-four measurement sites. He then drew streamlines and isotachs (contours of constant wind speed) for the twenty-six maps, checking maps individually and from hour to hour to insure consistency. We have subsequently reconstructed these maps, placing streamlines and isotachs for each hour on separate sheets to facilitate their use. Examples of these maps, for 7 AM, 10 AM, and 1 PM PST on 29 September 1969 (these times corresponding with those of the inversion maps shown in Figures C-10 to C-15) are presented in Figures C-17 to C-19 respectively.*

It was necessary, once the maps were prepared, to convert them to digital form, so that values of wind speed and direction might be stored in the computer for each of the 625 surface grid squares for each of the 26 hourly maps. As digitization is a substantial undertaking if carried out manually, we explored alternative possibilities. The one that appeared to have the greatest potential was the use of an interactive computer graphics system. Our hope was that it would be possible, through the use of a cathode ray tube (and light pen), tablet, or other input device, to enter the maps into computer memory. Appropriate computer software to be developed especially for this application would be required to convert the maps into the desired digital form. Retrieval of the data from memory would complete the conversion process.

---

*The maps presented in the Figures have been simplified for clarity of presentation and thus display a less dense array of isotachs and streamlines than appear in the actual maps.

Figures C-17 to C-19 follow.

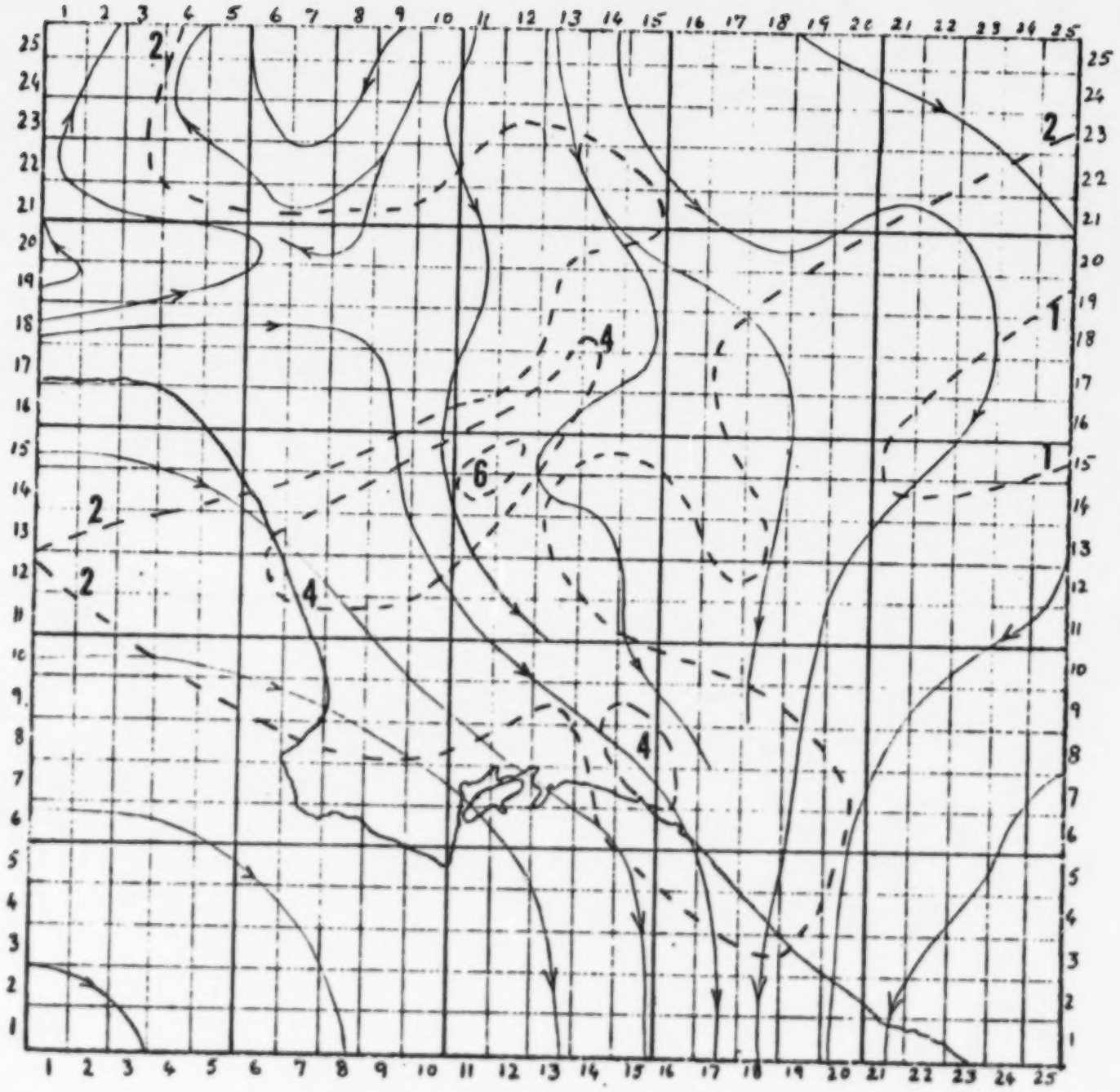

Streamlines

Isotachs (wind speeds given in miles per hour)

FIGURE C-17. Surface Wind Map for the Los Angeles Basin
29 September 1969
Averaging Period: 6:30 - 7:30 AM PST

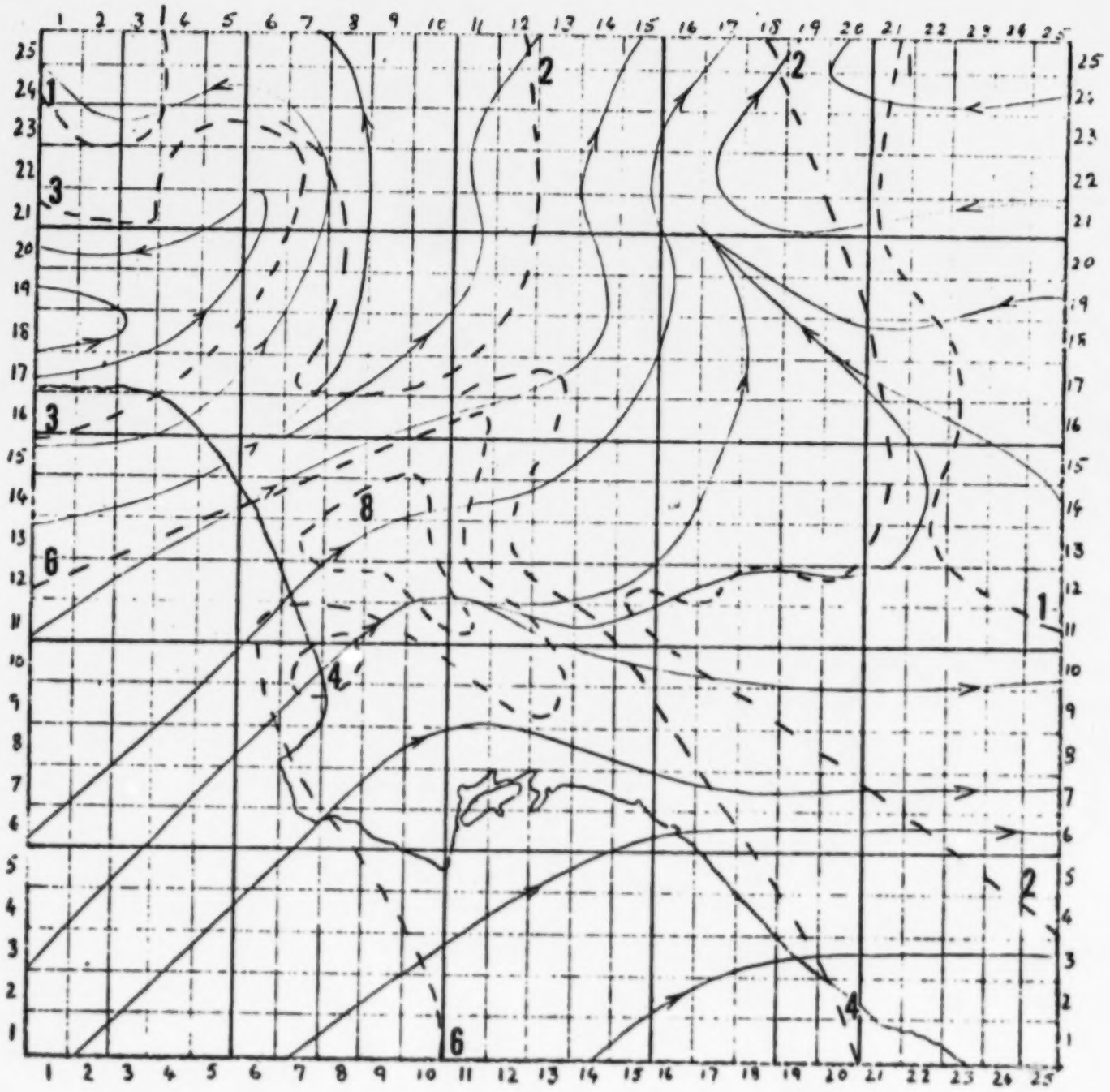

Streamlines
Isotachs (wind speeds given in miles per hour)

FIGURE C-18. Surface Wind Map for the Los Angeles Basin
29 September 1969
Averaging Period: 9:30 - 10:30 AM PST

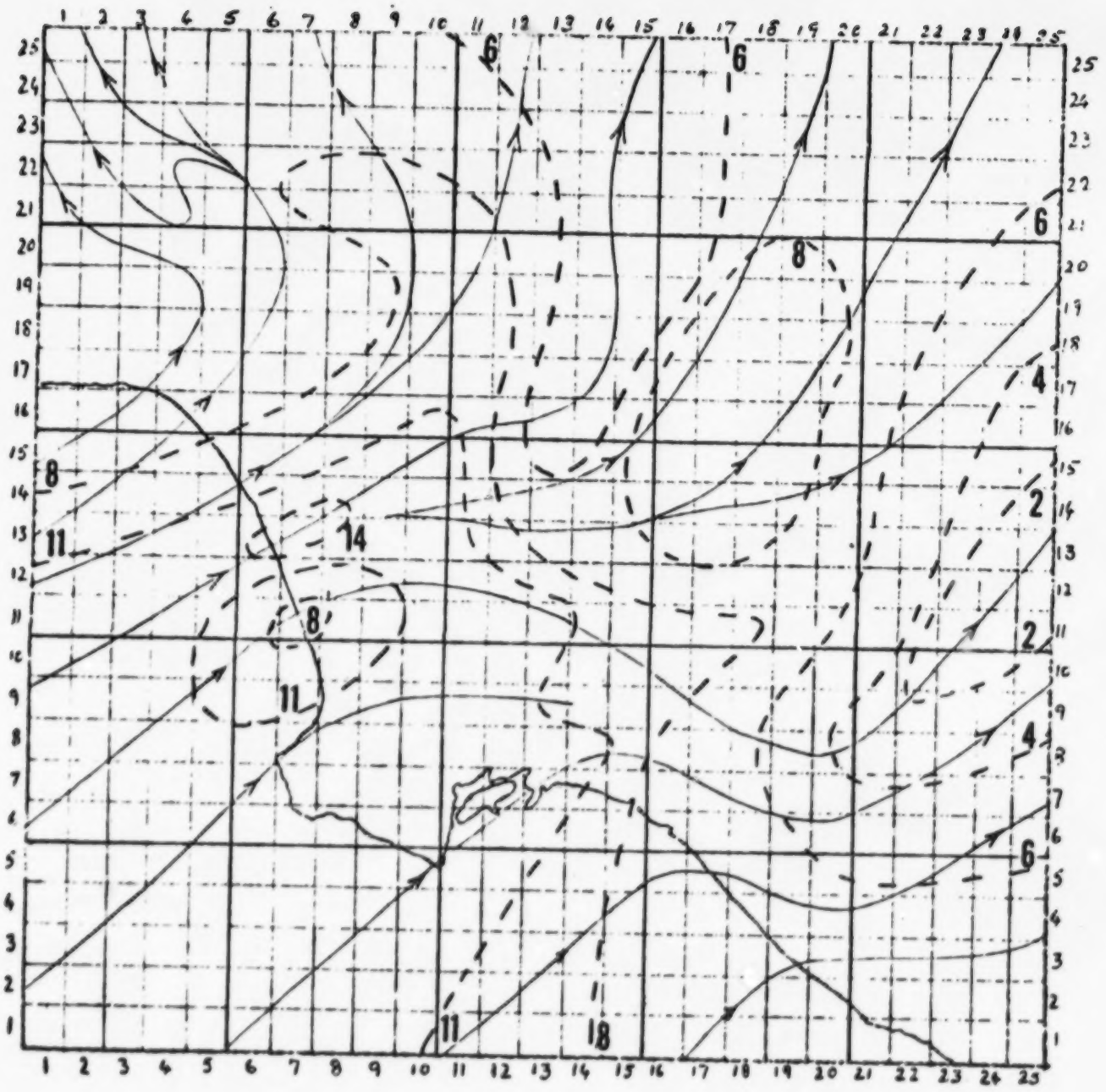

FIGURE C-19. Surface Wind Map for the Los Angeles Basin
20 September 1969
Averaging Period: 12:30 - 1:30 PM PST

Unfortunately, the time required for input of an individual map was quite a bit longer than expected--approximately an hour per map, and thus this mode of input proved to be unacceptably expensive. Input time could have been reduced substantially, but only through the mounting of a sizable software development program. Such an effort could have been justified only if a large number of maps were to be converted to digital form. Manual digitization of maps is much less expensive for the relatively small number we needed to convert, and was thus the procedure adopted. However, computer graphics remains an attractive future alternative. It is substantially less expensive per map if a large number of maps are to be converted to digital form on a routine basis. Furthermore, if a competent meteorologist operates the system, manual preparation of the maps can be carried out at the computer console, and thus the production of hard copy and the conversion to digital form can be accomplished simultaneously.

Manual digitization of the 26 maps involved several steps. Wind direction was measured at each square with a protractor; wind speed was read directly or interpolated by eye. The values were entered onto coding sheets, which were then used to prepare punched cards for actual input. Finally, these cards were checked for accuracy. It is apparent that this mode of data preparation is tedious and time consuming and requires several verification steps to minimize errors. While the manual procedure was justifiable both in terms of cost and time for the limited number of maps that were converted, automated methods of conversion will eventually be needed.

As we noted earlier, a computer graphics system is useful, both for the conversion of wind data to digital form and for the simultaneous preparation and digitization of maps. An alternative method for calculating wind speed and direction at each surface node point is the development and use of a computer-based interpolation procedure. A computer program for the computation of wind trajectories has been developed at Jet Propulsion Laboratory for the LACAPCD and, we are told, can be easily modified to compute streamlines and isotachs. Additional work is required, however, to take into account the effects of the Los Angeles Basin's complex topography.

In summary, we believe that automated methods for the preparation and digitization of surface wind are badly needed. Both the use of interactive computer graphics and the development of computer-based interpolation techniques should be explored as possible means for satisfying this need.

It is useful to close this section with a few comments pertaining to the wind data itself. Our experience thus far indicates that hourly representation of wind fields is probably satisfactory from overall considerations of accuracy. Furthermore, the existing measurement network of thirty-two stations scattered throughout the modeling region seems sufficiently dense to permit adequate representation of the wind field. However, the variation among stations in the mode of reporting data--in length of the averaging periods, in duration of measurement,

and in initial time of averaging period--creates an obvious problem in dealing with the data, a problem that could easily be eliminated by the adoption of a standard format (or formats). Finally, as we alluded to earlier, the relative inaccuracy of wind data collected during periods of low wind speed, largely due to the high thresholds characteristic of the monitoring equipment, can create serious difficulties in modeling. Monitoring equipment that is responsive to low speed air movements is badly needed.

III. WINDS ALOFT

One of the assumptions upon which the governing Equations (C-1) are based is that turbulent atmospheric flow is incompressible, i.e.,

$$\frac{\partial u}{\partial x} + \frac{\partial v}{\partial y} + \frac{\partial w}{\partial z} = 0 \qquad \text{(C-2)}$$

Unfortunately, the surface wind field, in general, does not satisfy this equation with w = 0. (Note that the vertical component of the wind, w, was not considered in Section II). In fact, if it is assumed that w = 0 everywhere and that the wind field aloft is identical to that at the surface (i.e., at each of the nine strata above the surface), the divergence of the surface wind field* produces an artificial inflation (or depression) of concentrations in the solution of Equations (C-1), an effect which is highly significant due to its cumulative nature. It is thus necessary that the entire wind field, however constructed, obey Equation (C-2).

Virtually no measurements are made of winds aloft. The only upper wind field data available for the validation period are those based on a tetroon program carried out by Pack, et al. (1970). One tetroon flight was made on 29 September and four on 30 September. Of these only three fall within the 6 AM - 6 PM PST modeling period. These data are obviously insufficient to serve as a basis for developing a description of winds above the surface.

In the absence of data, it was necessary to devise a means for constructing an elevated wind field. The following principles were observed in establishing a basis for the calculations:

1. Continuity must be satisfied for each cell in the 25 x 25 x 10 grid--i.e., inflow and outflow must be equal. Thus, for example, all w at the ground stratum should be chosen so that Equation (C-2) is satisfied for each cell in the layer.

2. The winds aloft, up to the base of the inversion, do not vary greatly in speed from winds at the surface. Wind directions do not vary significantly between the surface and the inversion base. (The latter assumption is undoubtedly violated, but in the absence of data, it is the safest assumption to make.)

3. Flow is smoother and less tortuous aloft than at the surface.

4. Flow through the inversion base is negligible. (Regions of wind convergence, such as the central San Fernando Valley, are an exception in that a continuous rising flow of air disrupts the inversion layer.) However, air from within the inversion layer

---

* If a mass balance is made over a portion of the surface wind field in x and y, there will typically be a net accumulation or depletion of material. Such a wind field is termed *divergent*.

mixes with marine air as the inversion base rises.

5. Lateral winds more or less follow the contours of the surface of the inversion base. (This effect is accounted for through the transformed Equations D-4.)

Following these guidelines, we considered two highly simplified approaches to establishing an upper wind field.

The first method is based on the assumption that $\frac{\partial u}{\partial z} = \frac{\partial v}{\partial z} = 0$, i.e., that the wind field aloft is identical to that at the ground. However, air is brought down through the inversion base, or released upward through it, as needed to satisfy continuity. Thus a vertical component of wind is calculated for each surface cell through a simple mass balance. If this component has magnitude $p(x,y)$, and if there are n horizontal strata of cells, the magnitude of this component for each column of cells is $np(x,y)$ at the inversion base and ip at the i^{th} stratum, counting from the ground (See Figure C-20c). This approach was applied in initial calculations and in the validation runs carried out early in the project. While this treatment is highly simplified and its shortcomings are apparent, it is nevertheless a convenient method for insuring that continuity is satisfied.

The second method that we have considered for constructing the wind field aloft combines the first method with a means for allowing flow variations in elevated strata. This approach represents an effort to satisfy continuity through the redistribution of air in the marine layer when divergence occurs at the surface. In this approach, it is assumed that a vertical wind component exists, and has the distribution shown in Figure C-20a. This is the equivalent of assuming that the horizontal wind vector has the distribution shown in Figure C-20b--in effect, two separate wind fields with a discontinuity. The surface wind field applies to the five lower strata; the wind field to be constructed applies to the five upper strata. Note the contrast between the vertical distribution of w assumed in this method and the distribution of w in the first method discussed, shown in Figure C-20c.

To calculate wind velocities in the elevated wind field for each column of cells, we seek a horizontal wind vector that does not vary more than $22\frac{1}{2}^{o}$ from the ground vector and that has a magnitude between one and two times that of the ground vector. (We wish to avoid unduly high wind speeds aloft, and at the same time, we expect that surface winds, hindered by resistance to flow at the ground, will be slower than those aloft). If this constraint cannot be satisfied through the redistribution of air from below the inversion base (at the same time, of course, satisfying continuity), we allow the entry of air from above (or flow upward) to an extent that the upper level horizontal wind speed and direction satisfy the following constraints:

1) Speed - within a factor of two of the surface wind speed in the same column of cells

2) Direction - within $22\frac{1}{2}^{o}$ of the surface wind direction in the same column,

Figure C-20 follows.

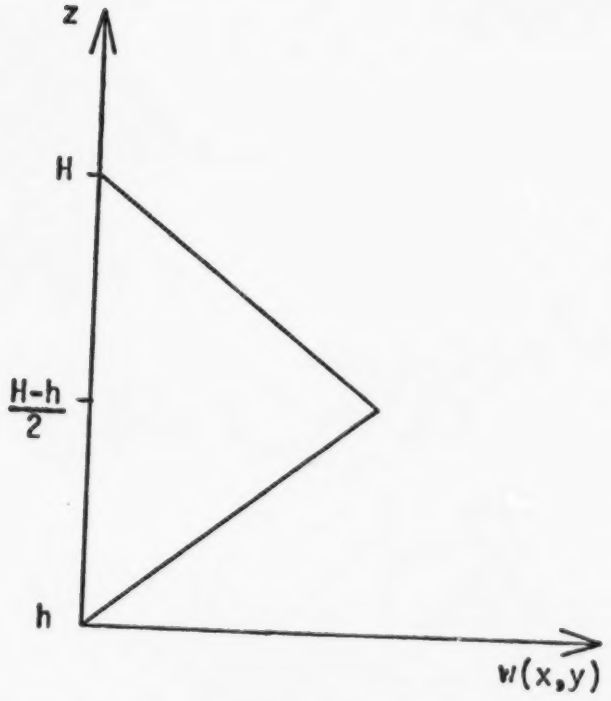

a. Assumed Vertical Distribution of w--Second Method (no air through inversion)

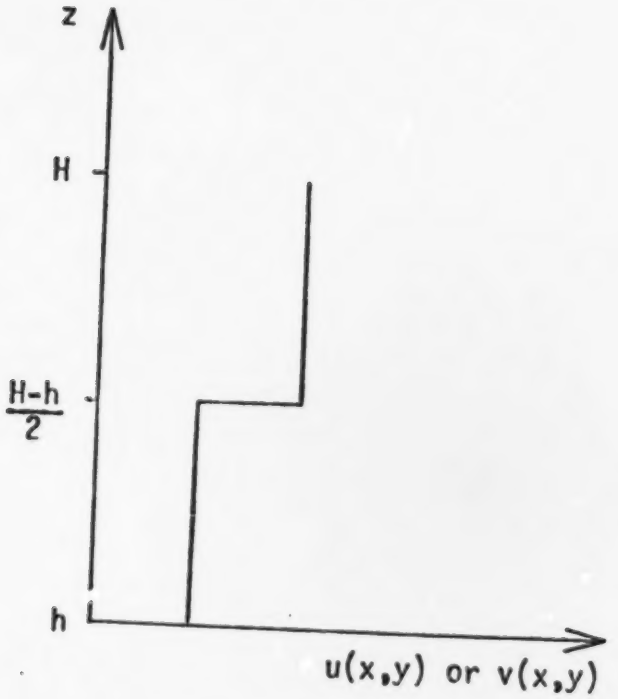

b. Vertical Distribution of u (or v)--Second Method

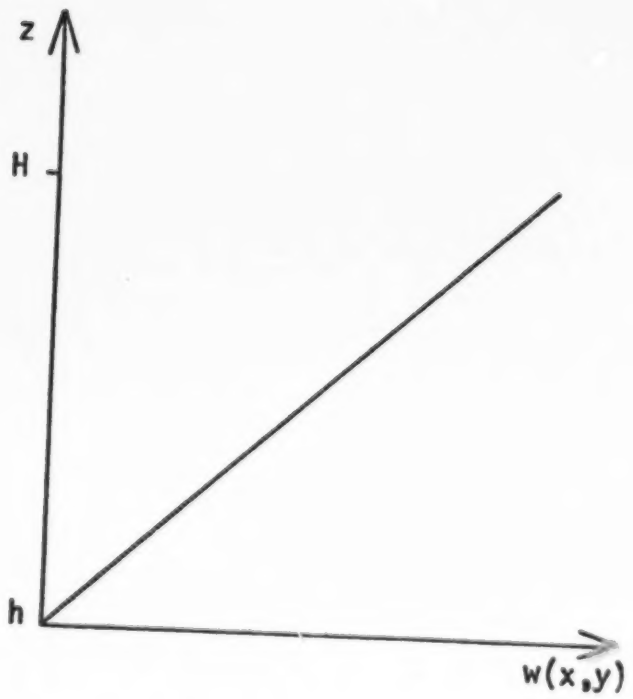

c. Assumed Vertical Distribution of w--First Method

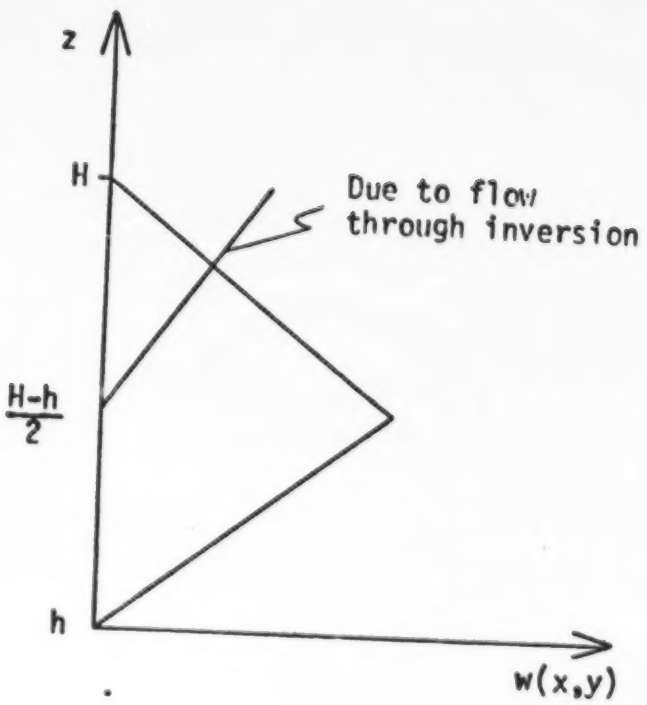

d. Assumed Vertical Distribution of w--Second Method (air permitted through inversion)

FIGURE C-20. Vertical Wind Velocity Profiles

at the same time minimizing the contribution of air through the inversion base. It should be noted that, in the event air is brought in from above the inversion base (or passed upward through it), the distribution of w is modified from that shown in Figure C-20a, becoming the sum of the distributions in Figure C-20d.

The actual calculation proceeds column by column, beginning at the southwest corner of the Basin, moving easterly until the southernmost row is completed, then continuing at the westernmost column of the second most southerly row. The calculation is dependent on the order in which it is carried out, as the calculated rate and direction of efflux from a column are the input variables to the next column. Comparisons were made of upper wind fields calculated beginning at the southwest and northeast corners of the modeling region.* In general, the two calculated wind fields were virtually the same in areas of smooth flow (over the ocean and the central and southern Basin), but tended to differ markedly over the San Gabriel Mountains, the San Fernando Valley, and a small portion of the Puente Hills. The wind field calculated beginning in the southwest corresponded to the surface wind field in a satisfying way, and this starting point was adopted.

In many ways this approach is rather appealing, based on physical considerations. Unfortunately, its development and incorporation into the main computer program did not take place until nearly the end of the work effort, and thus it has been the subject of only limited tests. We believe that its evaluation should be a part of future efforts.

---

* These comparisons were made using an earlier method of calculation, in which the opportunity to utilize air from above was much more restricted than in the approach described here. Thus, much poorer comparison was achieved in this test than would be expected in a test of the method actually described.

IV. TREATMENT OF TURBULENT DIFFUSIVITY

As horizontal turbulent diffusion has been neglected in the governing equations of continuity (C-1), it is necessary to consider only the vertical turbulent diffusivity, K_z, and its variation with elevation (z), with location (x,y), and with time (t). However, turbulent diffusivity is one of the more elusive quantities that must be estimated. It is not established through a direct measurement; it must be calculated from observed data. Furthermore, there is relatively little guidance available in the literature that is useful in estimating K_z. Thus, the accurate estimation of this parameter is currently virtually impossible.

Some useful *qualitative* observations can be made, however, regarding the turbulent diffusivity. K_z is a function of local velocity, shear field, and lapse rate; unfortunately, the functional relationship between K_z and these variables is largely unknown. In general, K_z increases approximately linearly with z near the ground. In the presence of an elevated inversion, however, we expect K_z to decrease with increasing z in the upper portions of the surface layer due to suppression of vertical buoyant fluctuations near the inversion base. Finally, values of K_z vary from about 300 ft.^{2}/minute under stable conditions to about 60,000 ft.^{2}/minute under unstable conditions.

Eschenroeder and Martinez (1969) reviewed the literature pertaining to the turbulent structure of the atmosphere and, based on this effort, adopted the following formulation for K_z (reported for 180 meter inversion base and 1 meter/second wind): 30 m^2/minute at the ground, increasing linearly to a height of 80 meters, at which height $K_z = 50(u+5)$ m^2/minute (u is the horizontal wind speed). K_z is held constant from 80 to 135 meters elevation, whereupon it decreases linearly to 30 m^2/minute at the inversion base. Based on this work, we have adopted a similar relationship:

$$K_z(x,y,z,t) = \begin{cases} 166.5[2-5\rho(x,y,z,t)] + \frac{5}{2}\rho(x,y,z,t)q(x,y,t) & 0 < \rho < 0.4 \\ q(x,y,t) & 0.4 < \rho < 0.8 \\ 333(5\rho(x,y,z,t) - 4) + 5[1-\rho(x,y,z,t)]q(x,y,t) & 0.8 < \rho < 1 \end{cases}$$

where

$$\rho(x,y,z,t) = \frac{z - h(x,y)}{H(x,y,t) - h(x,y)} \qquad \text{(C-3)}$$

$$q(x,y,t) = 500\left(\frac{\sqrt{u^2 + v^2}}{180} + 5\right)$$

and u,v = horizontal components of velocity (feet/minute)
K_z, q = turbulent diffusivities (square feet/minute)

The variation of K_z with z, as expressed in Equation (C-3), is shown schematically in Figure (C-21). Note that this relationship expresses the variation of K_z with z through the assumed form of the distribution, with x, y, and t through variations in the horizontal wind components with these quantities. However, the effects of shear field and vertical temperature structure are not considered in the formulation.

Figure C-21 follows.

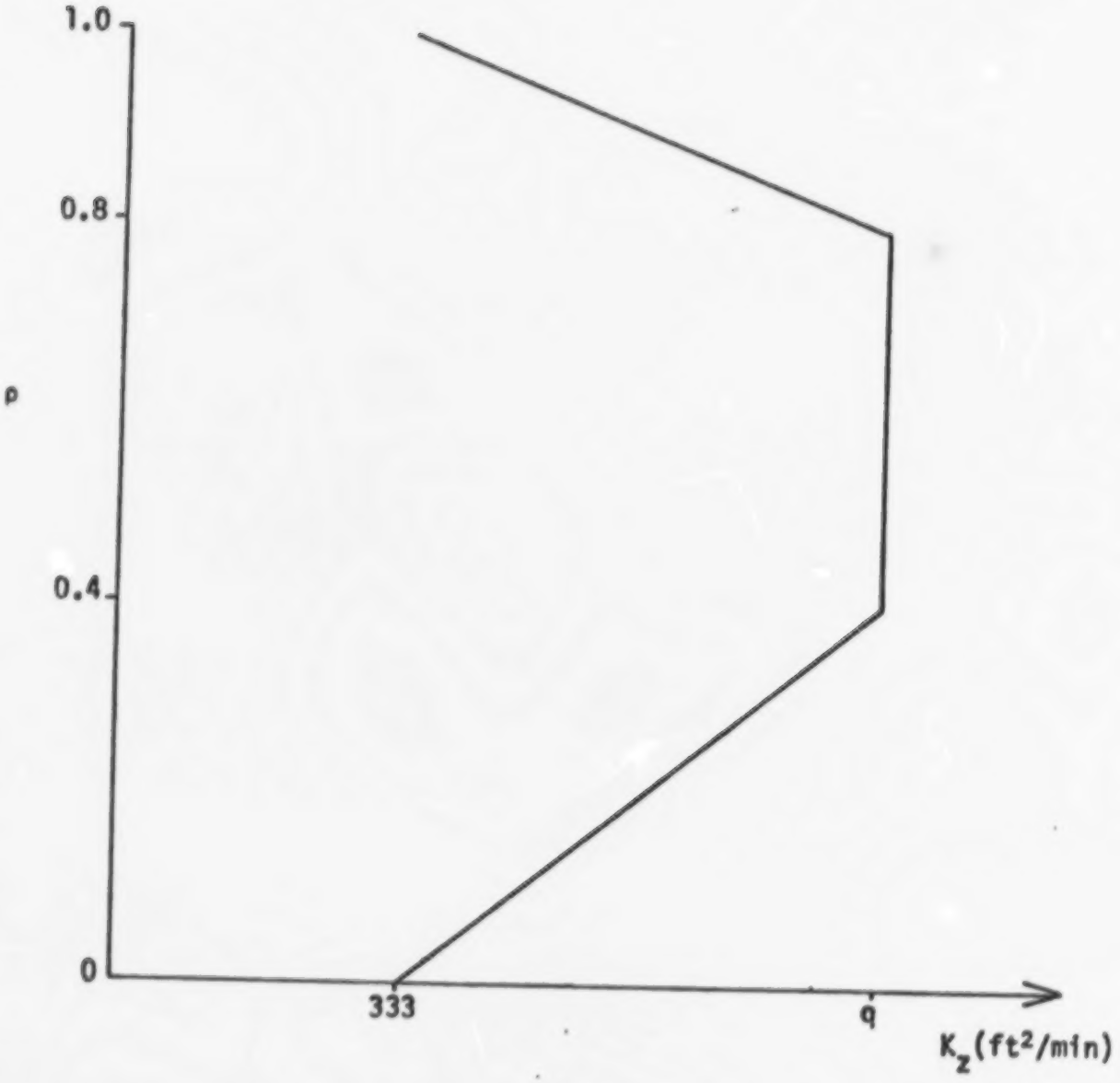

FIGURE C-21. Assumed Vertical Distribution of Turbulent Diffusivity, K_z

(For definitions of ρ and q, see Equation (C-3)).

This relationship has been applied in our validation runs to date. Calculations carried out thus far appear to be insensitive to modest variations in the form of the distribution. Much work is required, however, to properly include the effects of independent variables not considered here, and thus to better establish the functionality expressing turbulent diffusivity and its variations.

References

Bell, Gordon B., "A Study of Pollutant Transport Due to Surface Winds in Los Angeles, Orange, Riverside and San Bernardino Counties," State of California, Dept. of Public Health, Bureau of Air Sanitation (December 1969).

Edinger, James G., "Changes in the Depth of the Marine Layer Over the Los Angeles Basin," Journal of Meteorology, Vol. 16, No. 3 (June 1959), pp. 219-226.

Edinger, James G., and Roger A. Helvey, "The San Fernando Convergence Zone," Bulletin of the American Meteorological Society, Vol. 42, No. 9 (September 1961), pp. 626-627.

Eschenroeder, A. Q., and J. R. Martinez, "Mathematical Modeling of Photochemical Smog," General Research Corp., Santa Barbara, Calif., IMR 1210 (December 1969).

Neiburger, Morris, and James Edinger, "Meteorology of the Los Angeles Basin," Air Pollution Foundation, Los Angeles, California, Vol. 1, No. 1 (April 1954).

Neiburger, Morris, Nicholas A. Renzetti, and Rita Tice, "Wind Trajectory Studies of the Movement of Polluted Air in the Los Angeles Basin," Air Pollution Foundation, Los Angeles, California, Vol. 2, No. 1 (April 1956).

Pack, D. H., J. K. Angell, M. Hodges, W. Hoecker, and C. R. Dickson, "Tetroon Flights in Los Angeles, California - 1969," ESSA Technical Memorandum ERLTM-ARL 19, Air Resources Laboratories, Silver Spring, Md. (June 1970).

Panofsky, Hans A., "Air Pollution Meteorology," American Scientist, 57, 2, pp. 269-285 (1969).

Scott Research Laboratories, Inc., "Program Design and Methodology Data Summary and Discussion," 1969 Atmospheric Reaction Studies in the Los Angeles Basin, Final Report, Vol. 1 (Feb. 16, 1970).

Scott Research Laboratories, Inc., "Airborne Data ESSA Cooperative Data," 1969 Atmospheric Reaction Studies in the Los Angeles Basin, Final Report, Vol. IV (Feb. 16, 1970).